Human Molecular Genetics, 2003, Vol. 12, No. 14 ***1671–1687***
DOI: 10.1093/hmg/ddg184

ALS2, a novel guanine nucleotide exchange factor for the small GTPase Rab5, is implicated in endosomal dynamics

Asako Otomo[1,2], Shinji Hadano[1,2], Takeya Okada[2], Hikaru Mizumura[1], Ryota Kunita[1], Hitoshi Nishijima[3], Junko Showguchi-Miyata[2], Yoshiko Yanagisawa[1], Eri Kohiki[1], Etsuko Suga[1], Masanori Yasuda[4], Hitoshi Osuga[1,2], Takeharu Nishimoto[3], Shuh Narumiya[5] and Joh-E Ikeda[1,2,6,*]

[1]Solution Oriented Research for Science and Technology (SORST), Japan Science and Technology Corporation (JST), Tokai University School of Medicine, Isehara, Kanagawa 259-1193, Japan, [2]Department of Molecular Neuroscience, The Institute of Medical Sciences, Tokai University, Isehara, Kanagawa 259-1193, Japan, [3]Department of Molecular Biology, Graduate School of Medical Science, Kyushu University, Fukuoka 812-8582, Japan, [4]Department of Pathology, Tokai University School of Medicine, Isehara, Kanagawa 259-1193, Japan, [5]Department of Pharmacology, Kyoto University Faculty of Medicine, Kyoto 606-8501, Japan and [6]Department of Paediatrics, Faculty of Medicine, University of Ottawa, Ottawa, Ontario K1H 8M5, Canada

Received March 7, 2003; Revised and Accepted May 10, 2003

ALS2 **mutations account for a number of recessive motor neuron diseases including forms of amyotrophic lateral sclerosis, primary lateral sclerosis and hereditary spastic paraplegia. Although computational predictions suggest that *ALS2* encodes a protein containing multiple guanine nucleotide exchange factor (GEF) domains [RCC1-like domain (RLD), the Dbl homology and pleckstrin homology (DH/PH), and the vacuolar protein sorting 9 (VPS9)], the functions of the ALS2 protein have not been revealed as yet. Here we show that the ALS2 protein specifically binds to small GTPase Rab5 and functions as a GEF for Rab5. Ectopically expressed ALS2 protein localizes with Rab5 and early endosome antigen-1 (EEA1) onto early endosomal compartments and stimulates the enlargement of endosomes in cultured cortical neurons. The carboxy-terminus of ALS2 protein carrying a VPS9 domain mediates not only the activation of Rab5 via a guanine-nucleotide exchanging reaction but also the endosomal localization of the ALS2 protein, while the amino-terminal half containing RLD acts suppressive in its membranous localization. Further, the DH/PH domain in the middle portion of ALS2 protein enhances the VPS9 domain-mediated endosome fusions. Taken together, the ALS2 protein as a novel Rab5–GEF, ALS2rab5GEF seems to be implicated in the endosomal dynamics *in vivo*. Notably, a feature common to eight reported ALS2 mutations among motor neuron diseases is the loss of VPS9 domain, resulting in the failure of Rab5 activation. Thus, a perturbation of endosomal dynamics caused by loss of ALS2 rab5GEF activity might underlie neuronal dysfunction and degeneration in a number of motor neuron diseases.**

INTRODUCTION

ALS2 was initially identified as a causative gene for a juvenile recessive form of amyotrophic lateral sclerosis (ALS), termed ALS2 (OMIM 205100), in a Tunisian kindred, and a rare juvenile recessive form of primary lateral sclerosis (PLSJ; OMIM 606353) in both Kuwaiti and Saudi Arabian consanguineous families (1,2). ALS2 is characterized by a loss of upper motor neurons (UMN) and spasticity of limb and facial muscles occasionally associated with several signs of lower motor neuron (LMN) defects (3), whereas PLSJ shows only UMN symptoms with no evidence of denervation (4). Recently,

*To whom correspondence should be addressed at: Department of Molecular Neuroscience, The Institute of Medical Sciences, Tokai University, Isehara, Kanagawa 259-1193, Japan. Tel: +81 463915095; Fax: +81 463914993; Email: joh-e@nga.med.u-tokai.ac.jp

five independent homozygous *ALS2* mutations have been found in four families segregating an infantile-onset ascending hereditary spastic paralysis (IAHSP; OMIM 607225) (5,6) and a single family of a recessive complicated hereditary spastic paraplegia (HSP) (7). All of the *ALS2* mutations are either deletion or splicing site mutations (1,2,5,7). Current analysis of the genotype–phenotype correlations suggest that the truncation of the full-length ALS2 protein (a.k.a. alsin) resulting in the loss-of ALS2 function accounts for UMN degeneration, whereas the short variant of ALS2 resulting from an alternative splicing may be responsible for the phenotypic modulation, and possibly loss of both full-length and short ALS2 proteins might be related to the LMN defects (1,2,8).

Computational predictions have shown that the molecular mass of ALS2 protein (1657 amino acids) is 184 kDa, comprising several putative guanine nucleotide exchange factor (GEF) domains and motifs (1,2). A region in the amino-terminal half of the ALS2 protein is highly homologous to RCC1 (regulator of chromosome condensation) (9), and this is referred to as an RCC1-like domain (RLD) (10). RCC1 is a GEF for Ran (Ras-related nuclear) GTPase (9). The RLD is followed by the Dbl homology (DH) and pleckstrin homology (PH) domains, which are hallmarks for GEFs for Rho (Ras-homologous member) GTPases (11). The carboxy-terminal region contains a vacuolar protein sorting 9 (VPS9) domain, which has been found in a number of Rab5 (Ras-related in brain 5) GEFs including Vps9 (12), Rabex-5 (13), RIN1 (14,15) and RIN2 (16). In addition, eight consecutive MORN (membrane occupation and recognition nexus) motifs (17), whose repetition numbers have previously been reported as two (1) or seven (2), were noted in the region between PH and VPS9 domains.

The small GTPases control a broad spectrum of cellular and molecular processes. Ran GTPase is implicated in nuclear transfer as well as chromatin condensation through the regulation of microtubule assembly (18). The Rho subfamilies are critical regulators of the organization of the actin cytoskeleton (19,20), various signaling cascades (20,21) and neuronal morphogenesis (21–23). Further, the Rab GTPases have emerged as central players for vesicle budding, motility/trafficking and fusion (24). All of these small GTPases act as binary switches by cycling between an inactive (GDP-bound) and an active (GTP-bound) state. GEFs are known to stimulate the exchange of GDP for GTP, thereby generating the active forms of the small GTPases (25). In light of conserved GEF domains, it is tempting to speculate that the ALS2 protein acts as a regulator/activator of particular small GTPases. Notably, a feature common to eight reported mutations in *ALS2* is the loss of the carboxy-terminal VPS9 domain. Thus, a loss of VPS9-associated GEF function, which may result in the obstruction of membrane trafficking and dynamics, could underlie neuronal dysfunction and degeneration. However, none of the molecular features of the ALS2 protein has been revealed as yet, and mechanisms by which a loss of its function leads to a selective dysfunction and degeneration of motor neurons in motor neuron diseases (MNDs) remain unknown.

To delineate the functions of the ALS2 protein *in vivo*, biochemical and cell biological analyses were employed in this study. We demonstrate that the ALS2 protein specifically binds to small GTPase Rab5 and functions as a GEF for Rab5, but not for other 11 small GTPases. In addition, ectopically expressed ALS2 protein shows overlapping localization with either Rab5 or early endosome antigen-1 (EEA1) onto early endosomal compartments, and facilitates the enlargement of endosomes in cultured cortical neurons. The carboxy-terminus of ALS2 protein carrying a VPS9 domain activates Rab5 and mediates the endosomal localization of the ALS2 protein, while the amino-terminal half containing a RLD acts suppressive in its membranous localization. Further, DH/PH domain in the middle portion of the ALS2 protein retains an aggrandizing effect on the VPS9 domain-mediated endosome fusions. These data suggest that the ALS2 protein could function as a Rab5-GEF implicating in the endosome dynamics *in vivo*. The recent identification in a large consanguineous Pakistani HSP kindred of an *ALS2* deletion mutation at VPS9 domain (7) implies that the loss of functional VPS9 domain of the ALS2 protein is sufficient to cause neurodegeneration. Taken together, an obstruction of endosomal dynamics underlies neuronal dysfunction and degeneration in ALS2, PLSJ and HSP, as well as in a number of other MNDs.

RESULTS

The ALS2 protein is a 180 kDa protein and expressed in neurons

To detect the ALS2 protein in tissues, two independent polyclonal antibodies (HPP1024 and HPF1–680) were generated, and used to perform western blotting analysis. HPP1024 and HPF1–680 react with both human and mouse ALS2 proteins (Fig. 1A). Although several cross-reacting bands were observed, a major ~180 kDa common band was detected using these antibodies in mouse and human tissues (Fig. 1A), comparable to the molecular masses of 183 and 184 kDa predicted from murine and human ALS2 amino acid sequences, respectively. Thus, taking the180 kDa protein as the ALS2 protein reveals an expression in the brain that was highest in the cerebellum and lowest in the brain stem and spinal cord, where an expression pattern was similar to those of the *ALS2* mRNA as previously reported (1). Expression of the ALS2 protein in non-central nervous system (CNS) was generally low, except for in the liver, in which a 160 kDa protein, in addition to 180 kDa ALS2, was detected using two independent antibodies (HPP1024 and HPF1-680). Whether this 160 kDa protein represents a liver-specific ALS2 variant or a processed form of the intact ALS2 protein is unclear at this stage. The 180 kDa protein was also observed in the human cerebral cortex and cerebellum (Fig. 1A). No band corresponding to the previously described short ALS2 variant (1,2) was observed (data not shown).

Immunohistochemical analysis of the ALS2 protein using HPF1–680 combined with neuronal and glial markers revealed that the ALS2 protein is expressed in various neurons, but not glial cells (data not shown). Representative ALS2-immunoreactive staining of neurons from the motor area of the normal human cerebral cortex, which corresponds to the atrophic areas in the patient with *ALS2* mutation (6), was shown (Fig. 1B). The ALS2 protein mainly distributed in a diffused manner, but several dot or patchy stainings were consistently observed in

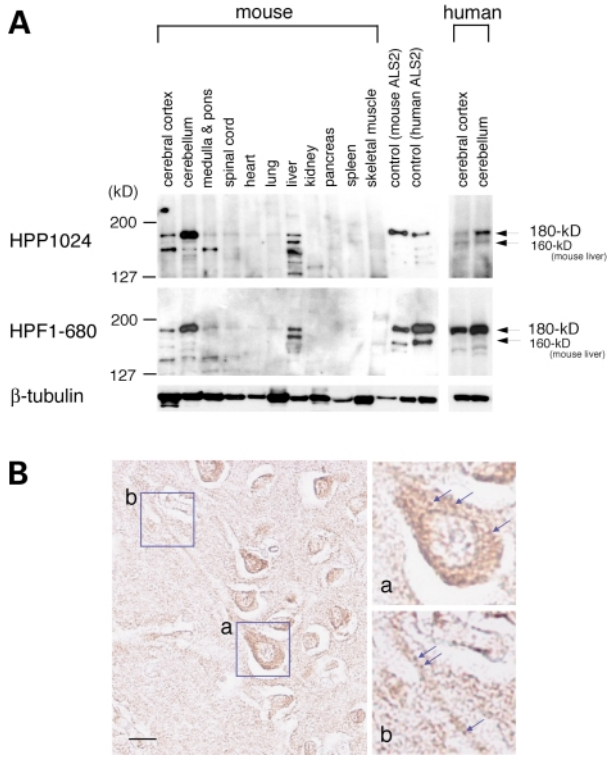

Figure 1. Western blotting and immunohistochemical analyses of the ALS2 protein expression in brain and other tissues in mice and human. (**A**) Western blotting analysis. Two different anti-ALS2 polyclonal antibodies (upper panel; HPP1024, middle panel; HPF1–680) were tested. As positive controls, protein extracts from the COS-7 cells ectopically expressing the full-length human or mouse ALS2 proteins were used. The lower panel represents the expression of β-tubulin to quantify the relative loading. Molecular mass markers are on the left. (**B**) Immunohistochemical analysis of the ALS2 protein using HPF1–680 antibody in the brain sections prepared from human cerebral cortex. The right-hand panels show the enlarged images of neuronal cell body (a) and dendrite (b), respectively. Arrows shown within these enlarged images indicate the typical dot-like stainings, which represent the vesicular localization for the ALS2 protein. Scale bars, 20 μm.

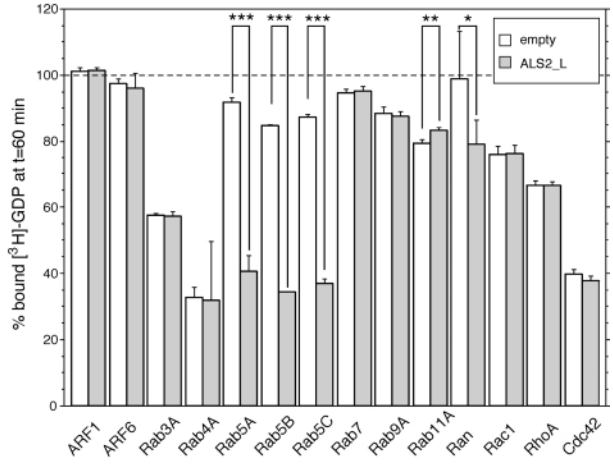

Figure 2. The full-length ALS2 protein accelerates GDP dissociation on members of Rab5 small GTPase family *in vitro.* A total of 14 small GTPases, including ARF1, ARF6, Rab3A, Rab4A, Rab5A, Rab5B, Rab5C, Rab7, Rab9A, Rab11A, Ran, Rac1, RhoA and Cdc42, were subjected to the *in vitro* GDP dissociation assay. Each [^{3}H]GDP-preloaded small GTPase was incubated with the immunoprecipitated FLAG-ALS2_L (gray bars) or FLAG-tag alone (empty; as a control, open bars) from COS-7 cells. The percentage of [^{3}H]GDP bound to each GTPase after 60 min is presented. Each value represents the mean and standard deviation of at least three independent assays. $***P < 0.0001$; $**P < 0.01$; $*P < 0.05$ in *t*-tests.

soma (Fig. 1B-a) as well as in dendrite (Fig. 1B-b), suggesting that the endogenous ALS2 protein localizes not only in the cytosol but also onto vesicular and/or membranous compartments in neurons.

The ALS2 protein acts as a Rab5-specific GEF

The ALS2 protein has been predicted to comprise three GEF domains: RLD, DH/PH and VPS9. To examine ALS2-associated GEF activities, *in vitro* GDP dissociation assays were performed using a variety of bacterially expressed small GTPases [Ran, Rab3A, Rab5A, ARF1 and ARF6 as candidates for RLD (10,26), Rac1, Cdc42 and RhoA as candidates for DH/PH (11), and Rab5A, Rab5B and Rab5C as candidates for VPS9 (12–16)]. Other small GTPases related to the membrane trafficking (24), such as Rab4A, Rab7, Rab9A and Rab11A, were also tested. Immunoprecipitated FLAG-tagged full-length ALS2 protein (ALS2_L) catalyzed [^{3}H]-GDP dissociation on Rab5A, Rab5B and Rab5C exclusively (Fig. 2). This suggests that ALS2_L possesses selective catalytic activity with all the members of Rab5 family. Although ALS2_L showed the weak Ran–GEF activity (Fig. 2), our preliminary assay with the amino-terminal RLD peptide of the ALS2 protein failed to detect any Ran-GEF activities (data not shown). Thus, the Ran-like GEF activity of ALS2_L remains unclear at this stage. In addition, none of the other small GTPases, including three well-characterized Rho-family small GTPases (Rac1, Cdc42 and RhoA) dissociated GDP by incubation with ALS2_L (Fig. 2). These data indicate that full-length ALS2 protein catalyzes GDP dissociation of Rab5 *in vitro*.

ALS2 MORN-VPS9 peptide retains the Rab5-GEF activity

In an effort to map the ALS2 functional domain which confers Rab5-GEF activity, ALS2rab5GEF, amino- and carboxy-terminally truncated ALS2 peptides were generated (Fig. 3A and B), and subjected to the *in vitro* GDP dissociation assay with Rab5A. GDP dissociation was observed with both incubation with full-length ALS2 (ALS2_L) as well as ALS2 peptides comprising 660–1657, 913–1657 or 1018–1657 amino acids, but not with ALS2 peptides of 1251–1657, 1351–1657 or 1–1275 amino acids (Fig. 3C). These results map the region conferring ALS2rab5GEF activity to the interval between 1018 and 1657 amino acids, corresponding to the MORN-VPS9 domains. Lack of either MORN motifs or VPS9 domain resulted in the loss of ALS2rab5GEF activity, indicating that both were necessary for the GEF activity *in vitro*.

To exclude the possibility that cofactors co-immunoprecipitated with ALS2-full length protein and peptides from COS-7 cell extracts were catalyzing the Rab5A-GDP dissociation, the assay was also conducted using bacterially produced GST-fusion ALS2 proteins. GST–ALS2_1018–1657 amino acids-dependent

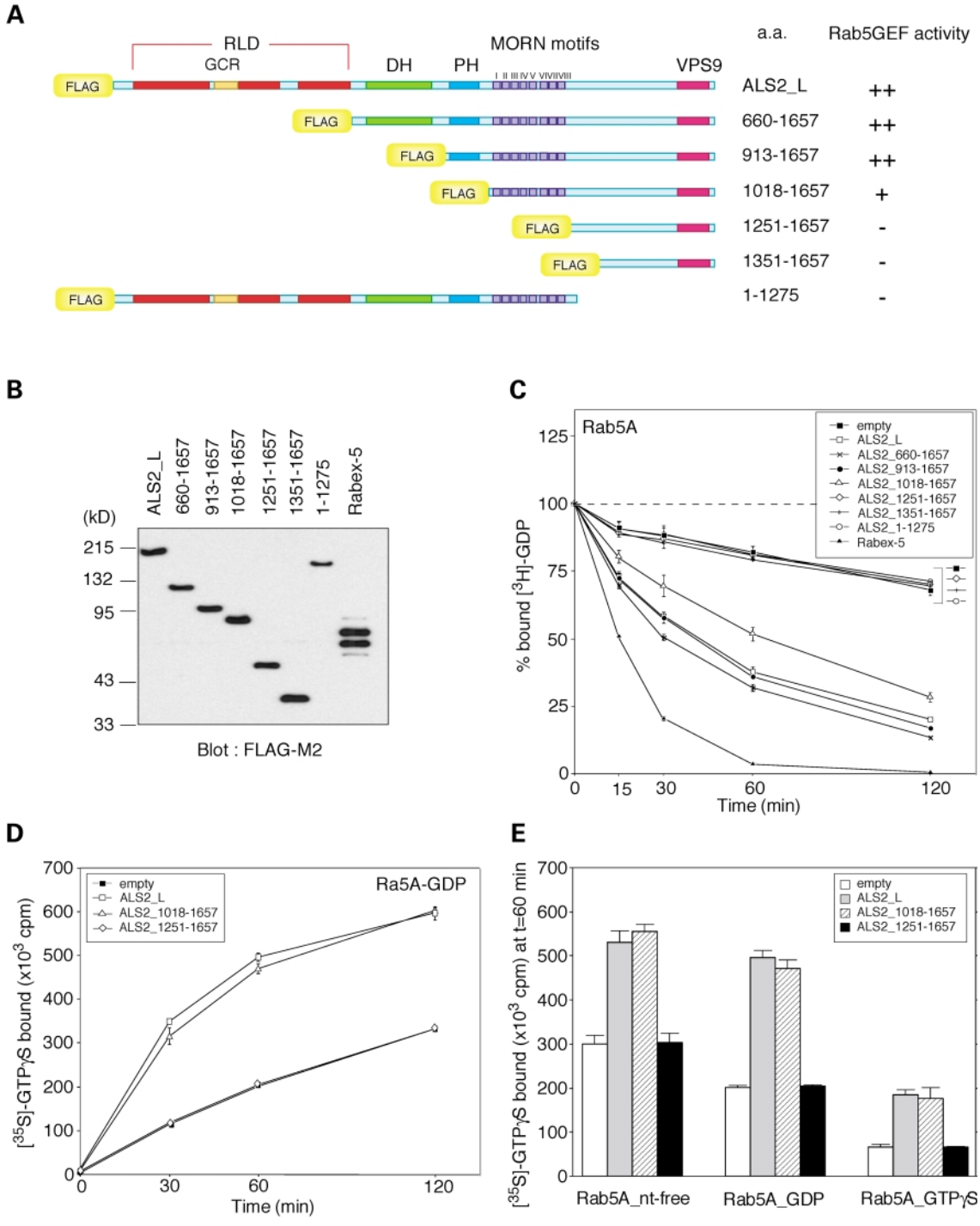

Figure 3. The MORN-VPS9 domain of ALS2 catalyzes Rab5 guanine nucleotide exchange reaction *in vitro.* (**A**) A schematic diagram of the domains and motifs of the ALS2 protein and various truncated mutant ALS2 peptides used for the GDP/GTP exchanging assays *in vitro.* RLD, RCC1-like domain, GCR, glucocorticoid receptor homologous region; DH, Dbl homology domain; PH, pleckstrin homology domain; MORN, membrane occupation and recognition nexus; VPS9, vacuolar protein sorting 9 domain. (**B**) Western blotting analysis of the immunoprecipitated FLAG-tagged full-length ALS2, various ALS2 fragments and Rabex-5 using FLAG-M2 monoclonal antibody. Equivalent amounts of recombinant proteins in the immunoprecipitates were subjected to the GDP/GTP exchanging assays *in vitro.* (**C**) The time-course of the [^{3}H]GDP dissociation on Rab5A induced by incubation with various ALS2 fragments. FLAG-tagged Rabex-5 was used as a positive control. The percentage of [^{3}H]GDP that remained bound on Rab5A at the indicated time points are shown. Each value represents the mean and standard error of three independent assays. (**D**) The time-course of the [^{35}S]GTPγS binding on the GDP-loaded Rab5A in the presence of a various fragments of ALS2. Each value represents the mean and standard error of three independent assays of the bound [^{35}S]GTPγS on Rab5A at the indicated time points. (**E**) Effect of the bound nucleotide-status for Rab5A on the *in vitro* [^{35}S]GTPγS binding activity catalyzed by the ALS2 protein and its truncated peptides. The nucleotide-free (Rab5A_nt-free), GDP-loaded (Rab5A_GDP) or GTPγS-loaded (Rab5A_GTPγS) Rab5A was incubated with [^{35}S]GTPγS in the presence of various ALS2 peptides for 60 min. Counts of the bound [^{35}S]GTPγS on Rab5A are presented. Each value represents the mean and standard deviation of at least three independent assays.

GDP-dissociation was observed, whereas neither GST–ALS2_1251–1657 nor GST–ALS2_1351–1657 amino acids revealed GEF activities with Rab5A (data not shown).

To confirm the ALS2rab5GEF activities, we next examined the ALS2 protein-dependent GTP–Rab5A complex formation by [^{35}S]GTPγS binding to Rab5A *in vitro*. The full-length (ALS2_L) as well as the MORN-VPS9 peptide (ALS2_1018–1657 amino acids) of the ALS2 protein actively exchanged the GDP molecule of the GDP-preloaded Rab5A for [^{35}S]GTPγS, and catalyzed [^{35}S]GTPγS · Rab5A formation in an incubation time-dependent (Fig. 3D). The ALS2 peptide lacking the MORN motifs, ALS2_1251–1657 amino acids, revealed no catalytic activity of either GTP exchange/loading or GDP-dissociation, confirming that the MORN-VPS9 domain spanned a minimum region for the ALS2rab5GEF function. ALS2rab5GEF, residing in the full-length or MORN-VPS9 peptide, actively loaded [^{35}S]GTPγS onto the GDP-bound Rab5A as well as nucleotide-free forms of Rab5A (Rab5A_GDP or Rab5A_nt free), while GTPγS-preloaded Rab5A molecules (Rab5A_GTPγS) were substrates with lower preferentiality (Fig. 3E).

The ALS2 protein interacts directly with Rab5

To examine whether the ALS2 protein directly interacts with Rab5, we carried out the *in vitro* binding assay using the FLAG-M2 pull-down experiment. The amino-terminally FLAG tagged full-length ALS2 protein bound to any form of Rab5A, including Rab5A_nt-free, Rab5A_GDP, and Rab5A_GTPγS, with the strongest binding to the nucleotide-free form of Rab5A (Fig. 4A). To examine the specificity for Rab5A binding and to refine the Rab5A binding region of the ALS2 protein, a series of GST-tagged ALS2-deletion constructs were generated and subjected to the GST pull-down experiments (Fig. 4B and C). GST–ALS2_1018-1657 amino acids, which spans a minimum region for ALS2rab5GEF activity, bound strongly to Rab5A, but not to either Rab4A or Rab11A (Fig. 4C), indicating that the binding is Rab5-specific. Further truncated ALS2 peptides, GST–ALS2_1251–1657 and _1351–1657 amino acids, showed weaker but reproducible Rab5A-binding activity (Fig. 4C), although both peptides no longer retain the GEF activities as mentioned above (Fig. 3C). Similar binding results were obtained from the yeast two-hybrid assay, in which ALS2_1351–1657 amino acids showed an interaction with Rab5A, while ALS2_1018–1351 amino acids, a peptide containing a consecutive MORN motif, did not (data not shown). Thus, a minimum region (1351–1657 amino acids) that needs to establish an interaction between the ALS2 protein and Rab5A is narrower and differs from the ALS2rab5GEF catalytic domain. Nevertheless, the steady interaction between ALS2_1018–1657 amino acids and Rab5A might be essential for the ALS2rab5GEF activity. All the ALS2 peptides tested in this assay showed selective bindings to any forms of Rab5A (Rab5A_nt-free, Rab5A_GDP and Rab5A_GTPγS; Fig. 4C).

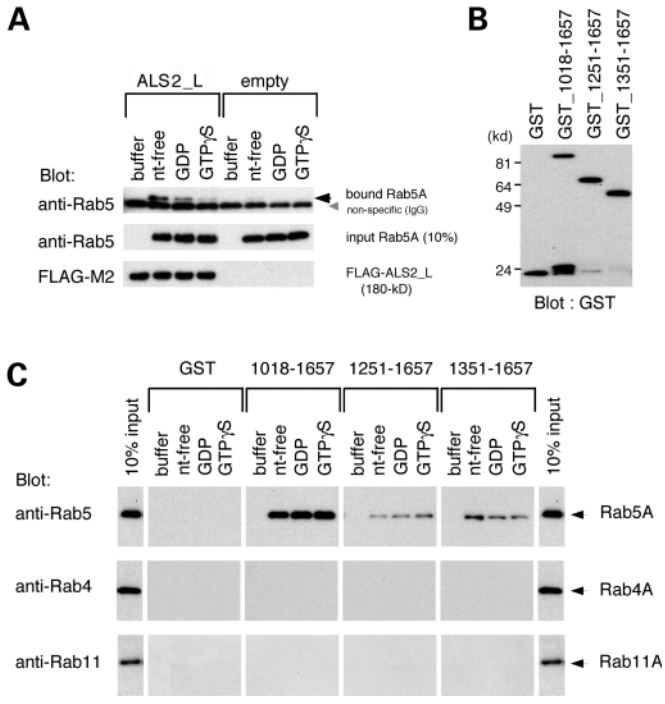

Figure 4. The carboxy-terminal portion of the ALS2 protein containing VPS9 domain is responsible for the direct interaction with Rab5A *in vitro*. (**A**) *In vitro* Rab5A binding assay using FLAG-tagged full-length ALS2. Nucleotide free (nt-free), GDP-bound (GDP), or GTPγS-bound (GTPγS) forms of Rab5A were incubated with FLAG-M2 beads conjugating FLAG-tagged full-length ALS2 (ALS2_L) or with FLAG-M2 beads alone (empty) as a control. The bound Rab5A was detected by immunoblotting method using anti-Rab5 antibody. Western blotting analyses of the input Rab5A and FLAG-tagged ALS2 were also conducted using anti-Rab5 and FLAG-M2 antibodies, respectively. (**B**) Western blotting analysis of the purified GST-fusion ALS2 peptides used in the GST pull-down assay. The positions of relative-molecular mass markers are shown on the left. (**C**) *In vitro* GST pull-down assay. Nucleotide free, GDP-bound or GTPγS-bound forms of Rab5A, Rab4A and Rab11A were incubated with glutathione–Sepharose 4B beads coupled with three different GST-fusion ALS2 peptides or with GST as a control. The bound Rab5A, Rab4A and Rab11A were detected by immunoblotting method using anti-Rab5, anti-Rab4 and anti-Rab11 antibodies, respectively. The '10% input' lanes show the western blotting analysis using 10% of the total amount of each Rab GTPase used in these binding experiments.

Ectopically expressed ALS2 protein exhibits overlapping distribution with Rab5 and EEA1 onto early endosome compartments

To investigate the sub-cellular localization of the ALS2 protein in detail, HeLa cells were transfected with expression construct expressing full-length and short form of the ALS2 proteins. Ectopically expressed short ALS2 variant distributed rather uniform in cytoplasm and nucleus with some dot-like stainings (Fig. 5A, ALS2_S). In contrast, when the full-length ALS2 protein was expressed, various patterns of the sub-cellular localizations were observed. By analyzing 500 cells expressing the full-length ALS2 protein, more than 90% of the cells harbored the ALS2 proteins in cytoplasm [Fig. 5A, ALS2_L (pattern 1)], while the ALS2 proteins in ∼6% of cells localized onto small vesicular structures in the perinuclear region [Fig. 5A, ALS2_L (pattern 2)], and were found the localization of ALS2 onto the enlarged vesicular structures in less than 1% of the cells [Fig. 5A, ALS2_L (pattern 3), arrow]. Interestingly, irrespective of the differences in distribution patterns, ∼20% of the cells revealed dense stainings at the leading edges or the cellular peripheries (Fig. 5A and B, arrowheads). To identify the organelles to which the ALS2 protein localized, co-localization

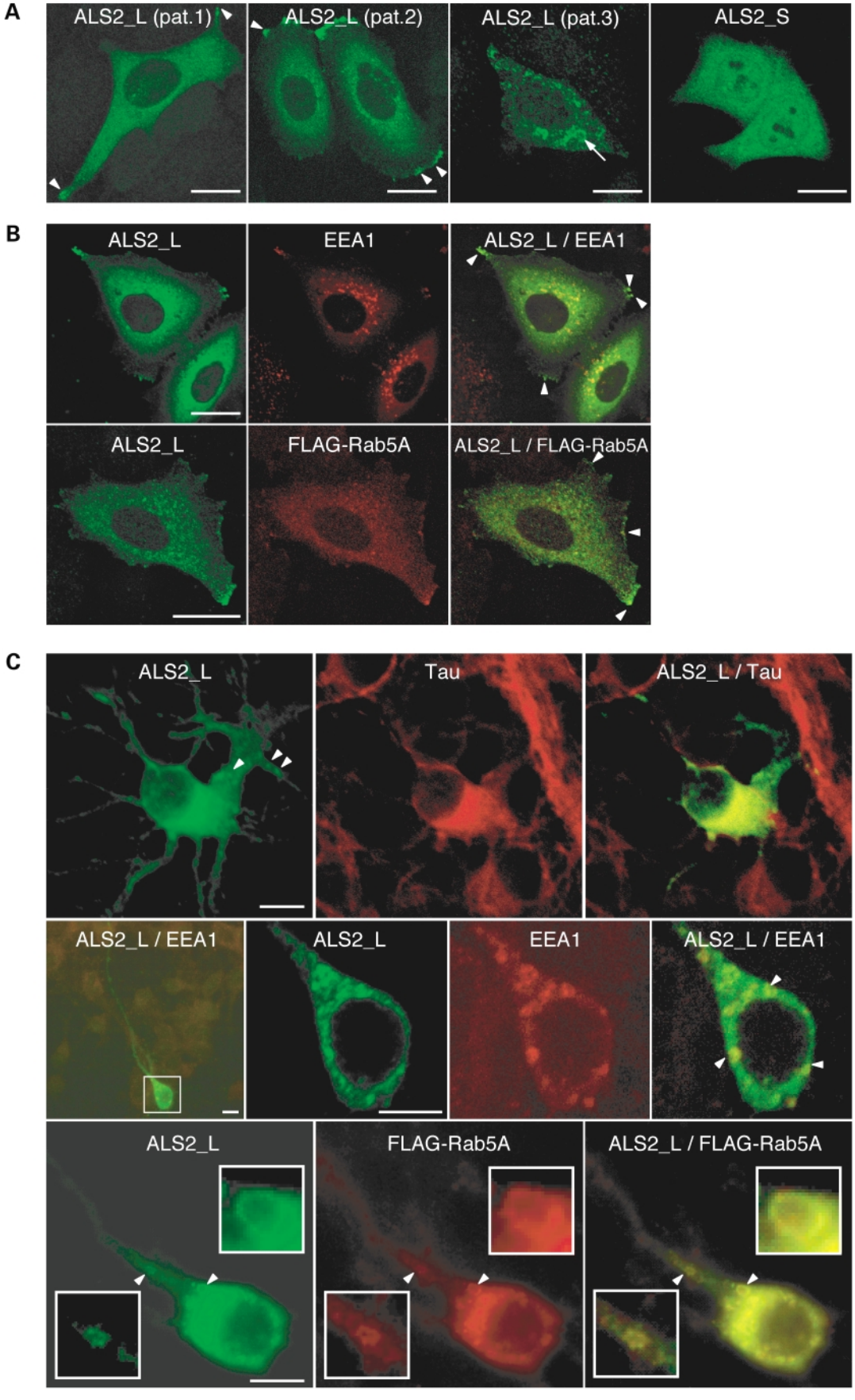
A
ALS2_L (pat.1)
ALS2_L (pat.2)
ALS2_L (pat.3)
ALS2_S
B
ALS2_L
EEA1
ALS2_L / EEA1
ALS2_L
FLAG-Rab5A
ALS2_L / FLAG-Rab5A
C
ALS2_L
Tau
ALS2_L / Tau
ALS2_L / EEA1
ALS2_L
EEA1
ALS2_L / EEA1
ALS2_L
FLAG-Rab5A
ALS2_L / FLAG-Rab5A

studies were conducted. Vesicular distributions of the ALS2 protein overlapped with those of endogenous EEA1, an early endosome marker (27) (Fig. 5B, ALS2_L/EEA1). Further, co-transfection of HeLa cells with expression constructs for the ALS2 protein and FLAG-tagged Rab5A demonstrated overlapped localization of the ALS2 protein with Rab5A onto the vesicular structures as well as cellular peripheries (Fig. 5B, ALS2_L/FLAG-Rab5A). These data indicate that a fraction of the ALS2 protein co-localizes with Rab5 onto the membranous compartments, particularly the early endosomes. Previous studies have shown that Rab5 acts cooperatively with EEA1 on early endosomes as a critical regulator in endosome fusions (28). Taken together, our findings imply a possible functional linkage between full-length ALS2 protein and Rab5 *in vivo.* Nonetheless, it is also evident that a majority of ALS2 molecules, at least in HeLa cells, exists in cytosol as possibly inactive or latent forms, because no obvious colocalization with Rab5 was observed (data not shown).

Overexpression of the ALS2 protein promotes endosome enlargement in cultured neuronal cells

To obtain further insights into the function of the ALS2 protein *in vivo*, rat primary cultured cortical neuronal cells were transfected with expression construct expressing the full-length ALS2 protein (Fig. 5C). It is noteworthy that the ectopically expressed ALS2 protein in Tau-positive neurons mostly spread throughout vesicles, which was in contrast to the diffused distributions in HeLa cells. We analyzed more than 100 neurons expressing the ALS2 protein, and ∼90% of the cells revealed vesicular/patchy stainings in soma as well as in the elaborated somato-dendritic neurites (Fig. 5C, ALS2_L/Tau). Further, ALS2 localization onto some enlarged vacuolar vesicles were also seen (∼10% of the cases; Fig. 5C, ALS2_L, arrowheads). A co-localization study with EEA1 demonstrated that the ALS2 protein localized onto EEA1-positive vesicular structures (Fig. 5C, middle panels; ALS2_L/EEA1), suggesting that the ALS2 protein functions on the early endosomal compartments in neurons (29). To obtain further evidence for the functional aspects of the ALS2 protein on early endosomes, co-transfection studies of cultured neuronal cells with expression constructs for the ALS2 protein and FLAG-tagged Rab5A were conducted. When the ALS2 protein and FLAG-Rab5A co-expressed, very enlarged endosomes, where the ALS2 protein coexisted with Rab5A, increased (Fig. 5C, ALS2_L/FLAG-Rab5A, arrowheads and enlarged images in the boxes), and those cells subsequently died prematurely. Taken together, overexpression of the full-length ALS2 protein in neuronal cells might promote endosome fusion/enlargement though the activation of the Rab5 within the endosomal compartments. Ectopic expression of a short variant of the ALS2 protein in cultured neurons revealed the diffused distributions in cytoplasm and nucleus (data not shown).

Molecular tropism and function for the ALS2 domains *in vivo*

To define the ALS2-domains responsible for the various subcellular localizations (diffused versus vesicular distributions), deletion constructs expressing the amino-terminally EGFP-fused ALS2 truncated mutants (Fig. 6A) were transfected into HeLa cells (Fig. 6B and C). EGFP-ALS2_1–680 amino acids carrying RLD showed a diffuse pattern of distribution with some patchy staining observed particularly in the perinulear area (Fig. 6B, EGFP_1–680), similar to the diffused-cases for full-length ALS2 (Fig. 6B, EGFP_ALS2L). Of particular note, a majority of the cases for EGFP-ALS2_660–1657 amino acids, containing the DH/PH/MORN/VPS9 region, revealed exclusive localization onto large-vacuolar structures (over ∼2 μm in diameter; Fig. 6B, EGFP_660–1657) and/or EEA1-positive vesicles (Fig. 6B, EGFP_660–1657/EEA1), which was reminiscent of the enlarged endosomes observed in cultured neuronal cells and the Rab5_Q79L (a constitutive active form)-expressing cells (Fig. 6B, FLAG–Rab5A_CA). It has been reported that overexpression of Rab5_CA resulted in the enlarged vesicles with a typical size of 2–5 μm (30). These data suggest that ALS2_660–1657 amino acid fragment constitutively activates the endogenous Rab5 and promotes the drastic enlargement of early endosomes. EGFP-ALS2_1018–1657 amino acid (MORN/VPS9 domains), spanning a minimum region for the ALS2rab5GEF activity, also preferentially localized onto the EEA1-positive endosomes with the marginal enlargement (less than ∼2 μm in diameter; Fig. 6B, EGFP_1018–1657/EEA1). The result was very similar to that obtained by the overexpression of the FLAG-tagged Rabex-5 (Fig. 6B, FLAG-Rabex-5). Further, EGFP-ALS2_1351–1657 amino acid fragments, lacking the Rab5-GEF activity, showed the similar degree of the vesicular localizations (Fig. 6B, EGFP_1351–1657). Consistent results were obtained for amino-terminally FLAG-tagged or the carboxy-terminally EGFP-fused ALS2 molecules in both COS-7 and HeLa cells (data not shown). These data suggest that each ALS2 domain/region demonstrates specific subcellular tropism *in vivo* (Fig. 6C). The amino-terminal RLD seems to confer cytosolic distribution, and thus could function as a negative regulator for the Rab5 binding and activation of Rab5. In contrast, the carboxy-terminus containing the VPS9 domain might mediate both Rab5 binding and endosomal localization. Notably the DH/PH constitutively promotes the MORN/VPS9-mediated Rab5

Figure 5. Ectopically expressed ALS2 showed overlapping distribution with Rab5 and EEA1 onto early endosome compartments in HeLa and rat cultured cortical neuronal cells. (**A**) Subcellular distribution of the ectopically expressed full-length (ALS2_L) or short form (ALS2_S) of the ALS2 proteins in HeLa cells. Three patterns of the ALS2 distributions are shown: patterns 1, 2, and 3. Arrowheads indicate the dense ALS2 stainings at the leading edges. The arrow indicates the ALS2 localization onto the enlarged vesicular structures. (**B**) Co-localization of ALS2_L with EEA1 or FLAG-tagged Rab5A. Left, middle and right columns represent ALS2_L, EEA1 or FLAG_Rab5A, and each merged image, respectively. Arrowheads indicate the dense ALS2 stainings at the leading edges or the cell peripheries. (**C**) Ectopically expressed full-length ALS2 in rat primary cortical neurons. The ALS2, EEA1, FLAG-tagged Rab5A and Tau proteins were immunofluorescently detected using anti-ALS2 polyclonal antibody (HPF1–680), anti-EEA1 monoclonal antibody FLAG-M2 monoclonal antibody and anti-Tau monoclonal antibody, respectively. Arrowheads indicate the ALS2 localization onto the enlarged vesicular structures. All the images were obtained by processing for immunofluorescence and analyzing by laser scanning confocal microscopy. Scale bars, 10 μm.

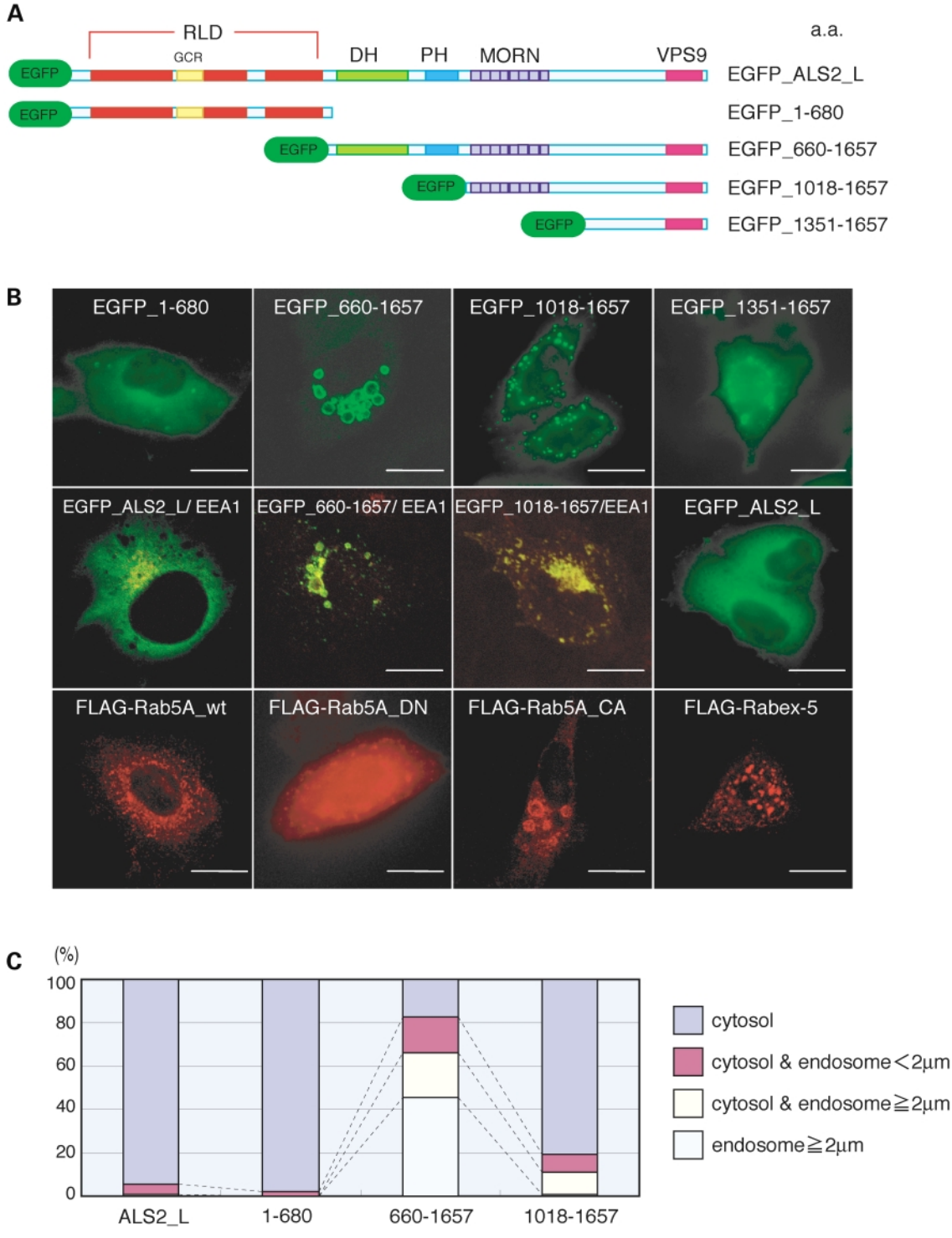

Figure 6. The ALS2 domains show distinct subcellular localizations and effects in HeLa cells. (**A**) A schematic diagram of the ALS2 protein and its truncated mutants used in the localization study. (**B**) Subcellular distribution of the ectopically expressed EGFP-fused proteins carrying distinct portions of ALS2 (EGFP–ALS2_1–680, EGFP–ALS2_660–1657, EGFP–ALS2_1018–1657, EGFP–ALS2_1351–1657 amino acids), full-length ALS2 (EGFP–ALS2_L), FLAG-tagged Rab5A [FLAG–Rab5A_wt (wild type), Rab5A_DN (dominant negative type; S34N), and Rab5A_CA (constitutive active type; Q79L)], and FLAG-tagged Rabex-5 in HeLa cells. Co-localization of the ALS2 fragments with endogenous EEA1were also shown (EGFP–ALS2_L/EEA1, EGFP_660–1657/EEA1 and EGFP_1018–1657/EEA1). All the images were obtained by processing for immunofluorescence and analyzing by laser scanning confocal microscopy. Scale bars, 20 μm. (**C**) Subcellular localization of the full-length and truncated ALS2 proteins and their effects on sizes of the ALS2-positive vesicular structures. Five hundred cells expressing each EGFP-fused ALS2 fragment were analyzed and counted. The percentages of the cell numbers revealing each localization phenotype are shown. The cells that showed the diffused ALS2 distributions were counted as 'cytosol'. The cells that showed vesicular ALS2 distributions were classified into two groups: 'endosome (<~2 μm)' represents the cells containing all the vesicles with less than ~2 μm in diameter (no and/or marginal enlargement); and 'endosome (≥~2 μm)' represents the cells revealing at least one of the vesicles with over ~2 μm in diameter (significant enlargement).

activation and endosome fusions *in vivo*, indicating the ALS2_660–1657 amino acid peptide might be a constitutive-active form for ALS2rab5GEF in the cells. Taken together, the Rab5-GEF activity associated with the full-length ALS2, ALS2rab5GEF, seems to be controlled by an internal domain(s) of ALS2 and implicated in the endosome dynamics *in vivo.*

Effect of the overexpression of the constitutive active form of the ALS2 protein on endosome dynamics

To delineate the molecular aspects of the ALS2rab5GEF activity on endosomal dynamics, we adopted overexpression of the ALS2_660–1657 amino acid peptide, a constitutive-active form for ALS2rab5GEF, in HeLa cells as a model system for the ALS2-activating status.

First, we examined the subcellular distribution of ectopically expressed ALS2_660–1657 amino acids. Co-localization was assessed with several other Rab family GTPases including Rab4A as early endosome markers (31,32), Rab7 as a late endosome marker (31,33,34) and Rab11A as a recycling endosome marker (31,35) (Fig. 7A). Co-transfection of HeLa cells with expression constructs for EGFP–ALS2_660–1657 amino acids and FLAG-tagged Rab4A, Rab7 and Rab11A demonstrated ALS2 protein co-localization with Rab4A (Fig. 7A, EGFP_660–1657/FLAG-Rab4A) and partially with Rab7 (Fig. 7A, EGFP_660–1657/FLAG-Rab7), but not with Rab11A (Fig. 7A, EGFP_660–1657/FLAG-Rab11A), indicating that ALS2_660–1657 amino acid peptide localizes predominantly onto the early endosome compartment and less frequently onto the late endosome, but not onto recycling endosome. ALS2_660–1657 amino acids did not localize to Golgi compartments by assessing the colocalization with GM130, a *cis*-Golgi marker (36) (data not shown).

To study whether the overexpression of ALS2_660–1657 amino acids affects endocytosis, HeLa cells transfected with ALS2_660–1657 amino acids expression construct were cultured in the presence of transferrin (Tfn) and epidermal growth factor (EGF), respectively, and distributions of these proteins within the cells were analyzed. ALS2_660–1657 amino acid and either Tfn or EGF predominantly co-localized onto the large vesicular compartments (Fig. 7B), consistent with the localization of the ALS2 peptides onto the actively internalized/endocytosed membrane compartments within the cells. On the other hand, ALS2_660–1657 amino acid peptide non-expressing cells observed in the same microscopic field only showed smaller Tfn- or EGF-positive vesicles without any evidence for endosome enlargement (Fig. 7B). These data also imply that overexpression of ALS2_660–1657 amino acids does not obstruct endocytosis of either Tfn or EGF, although it is still not clear whether trafficking of these molecules is disturbed within the cells.

To obtain insight into the effect of ALS2_660–1657 amino acids on the early/late endosomal dynamics, the distributions of two endosomal marker proteins, LAMP-1 and LAMP2, which were known as late endosome/lysosome markers (37,38), in cells expressing ALS2_660–1657 amino acids were analyzed. Overexpression of ALS2_660–1657 amino acids was associated with the accumulation of the lysosomal-associated membrane proteins LAMP-1 and LAMP-2 within the enlarged early endosome compartments (Fig. 7C). These data suggest an

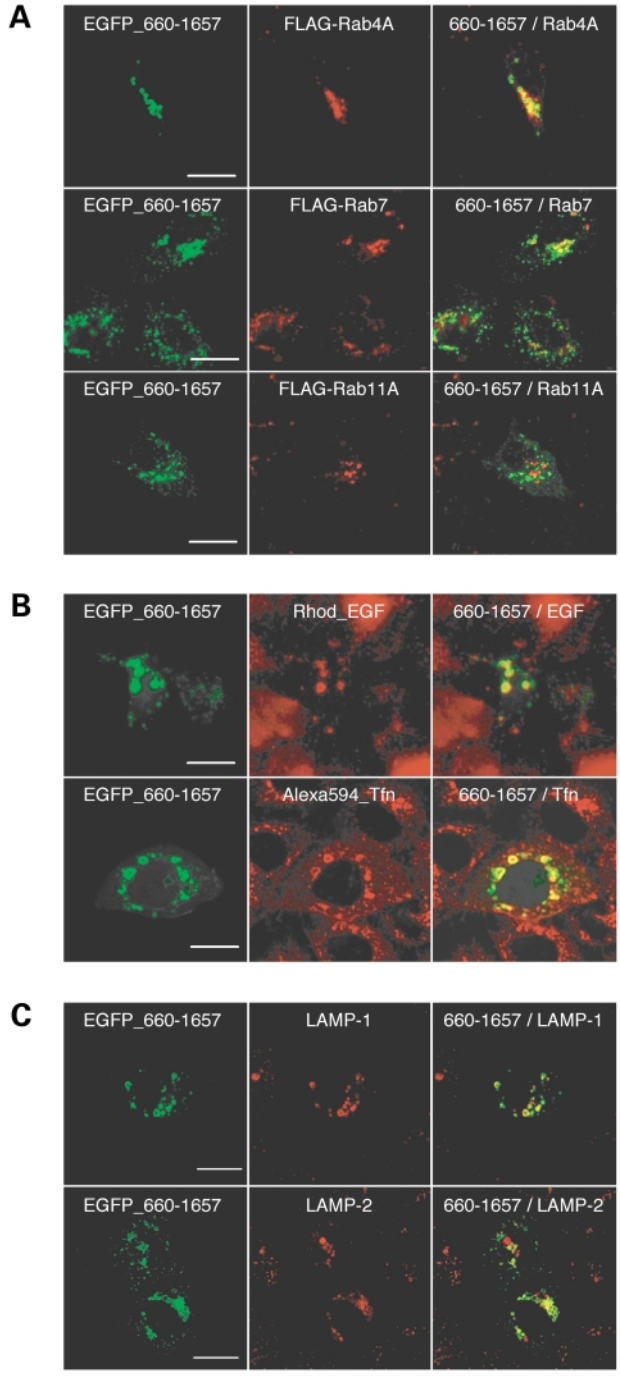

Figure 7. Effects of overexpression of ALS2_660–1657 amino acid peptide containing DH/PH domains on endosome dynamics in HeLa cells. (**A**) Confocal microscopic images of the HeLa cells ectopically co-expressed EGFP–ALS2_660–1657 amino acids (left-hand columns) and FLAG-tagged Rab family small GTPases (middle columns): FLAG-Rab4A, FLAG-Rab7 and FLAG-Rab11A. The right-hand columns display the merged images. (**B**) Colocalization of EGFP–ALS2_660–1657 amino acids (left-hand columns) and endocytic tracers; tetramedtylrhodamine-conjugated EGF (Rhod_EGF) (upper middle column) and Alexa 594-conjugated transferrin (Alexa594_Tfn) (lower middle column) onto enlarged endosomes in HeLa cells. Merged images are on the right. (**C**) Confocal microscopic immunofluorescence images for the ectopically expressed EGFP–ALS2_660–1657 amino acids (left-hand columns) and the endogenous organelle marker proteins (middle columns), including LAMP-1 (late endosome) and LAMP-2 (late endosome/lysosome) in HeLa cells. The right-hand columns display the merged images. Scale bars, 20 μm.

obstruction of lysosomal protein trafficking (39), possibly as a result of endosomal enlargement.

VPS9 domain functions as Rab5–GEF and contributes to the endosomal localization of the ALS2 protein

Given that protein sequence in the carboxy-terminal of the ALS2 protein functions as Rab5-GEF and localizes onto the enlarged endosome compartments, it was of particular interest to know whether the ALS2 protein is directly involved in endosome dynamics. We generated amino acid substituted mutants in which well-conserved amino acid residues among several VPS9 containing proteins were mutated (Fig. 8A): ALS2_660–1657 amino acid (P1603A) (proline at position 1603 to alanine) and ALS2_660–1657 amino acid (L1617A) (leucine at position 1617 to alanine). First, we assayed the GEF activity and GDP dissociation *in vitro* of these mutant proteins in the presence of Rab5A. Both mutations resulted in a marked decrease in GDP dissociation (Fig. 8B), implying that these amino acid residues are essential for ALS2rab5GEF activity. Next, we studied a subcellular localization of the ectopically expressed amino-terminally EGFP-fused mutant proteins in HeLa cells. EGFP–ALS2_660–1657 amino acids (P1603A) localized to as the same subcellular compartments as EGFP–ALS2_660–1657, _1018–1657 and _1351–1657 amino acids, without the enlargement of endosomes [Fig. 9A, EGFP_660–1657(P1603A)]. This suggests that ALS2_660–1657 amino acids (P1603A) fails in the endosome fusion by the loss of its GEF activity, although the mutant protein is recruited onto the endosomal compartments. By contrast, the EGFP–ALS2_660–1657 amino acids (L1617A) mutant scattered in cytosol [Fig. 9A, EGFP_660–1657(L1617A)], indicating that the L1617A mutation causes a loss of both ALS2rab5GEF activities and migration to the endosomal compartments.

ALS2 protein-induced enlargement of endosomal compartments is mediated by the activation of Rab5-EEA1 pathway

To examine whether ALS2_660–1657 amino acids directly activates small GTPase Rab5 and is involved in endosomal dynamics *in vivo*, co-expression experiments were undertaken with Rab5 proteins in HeLa cells. Transient expression of Rab5A_Q79L (constitutively active mutant) promoted the enlargement of endosomal compartments, while that of either Rab5A wild-type or Rab5A_S34N (dominant-negative mutant) provided the small and punctate vesicles (Fig. 6B, FLAG-Rab5A_wt or FLAG-Rab5A_DN), as reported previously (29,31,32). Co-expression of Rab5A_wt and ALS2_660–1657 amino acids revealed a prominent enlargement of endosomes (Fig. 9B, 660–1657/Rab5A_wt), indicating that the ectopically expressed Rab5A could be activated by ALS2rab5GEF to promote further enlargement of endosomes. This stimulatory effect was not seen when Rab5A_wt was co-expressed with ALS2_660–1657 amino acids (P1603A) [Fig. 9A, 660–1657(P1603A)/Rab5A_wt] or ALS2_660–1657 amino acids (L1617A) [Fig. 9A, 660–1657(L1617A)/Rab5A_wt]. Thus, the enlargement of endosomal compartments correlated closely with the activation of Rab5 GTPase by ALS2rab5GEF, suggesting a role for this protein in endosomal trafficking and

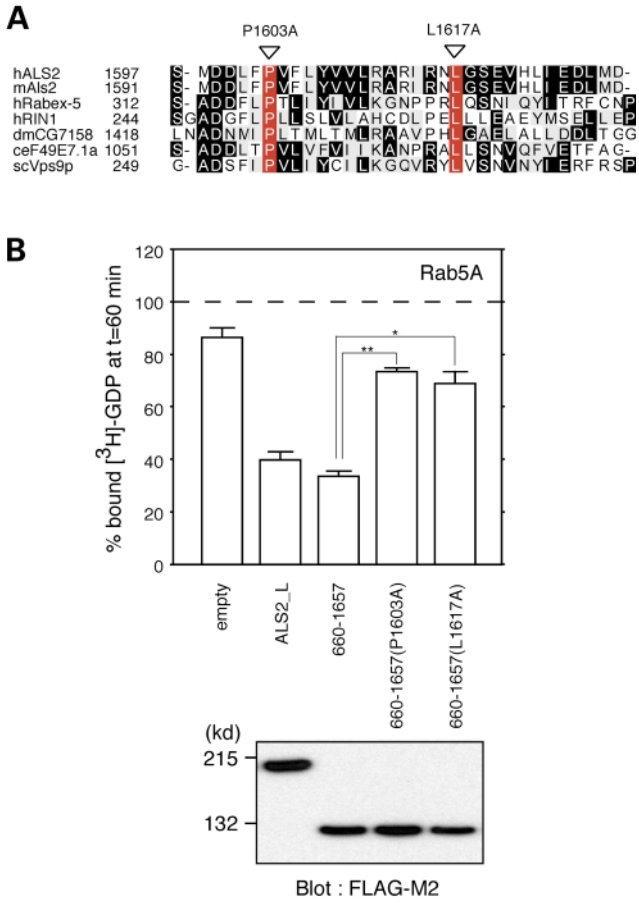

Figure 8. Effects of mutations in the VPS9 domain of the ALS2 protein on Rab5-GEF activity *in vitro*. (**A**) Multiple alignment of a portion of the VPS9 domains in the deduced ALS2 protein sequence. For VPS9 domains, human ALS2 (hALS2_VPS9), mouse ALS2 (mALS2_VPS9), human Rabex-5 (hRabex-5, ref; NP_055319), human Ras inhibitor RIN1 (hRasinhibitor, ref; NP_004283), *D. melanogaster* CG7158 (dmCG7158, gb; AAF51764), *C. elegans* F49E7.1a (ceF49E7.1a) and *S. cerevisiae* Vps9p (scVps9p, ref; NP_013612) are aligned. The black and gray shading represents identical and conserved amino acids, respectively. Sequences are numbered with the initiation codon of each protein as no. 1. The red shading represents the amino acids mutated in this study. (**B**) The [^{3}H]GDP dissociation assay *in vitro* using mutant ALS2 proteins: ALS2_660–1657, ALS2_660–1657(P1603A) and ALS2_660–1657 amino acids (L1617A). Western blotting of the immunoprecipitated FLAG-tagged ALS2 and its mutants used in this study are also shown. The percentage of [^{3}H]GDP that remained bound to Rab5A after 60 min is presented. Each value represents the mean and standard deviation of at least three independent assays. $^{**}P < 0.0001$; $^{*}P < 0.001$ in *t*-tests.

fusion via activation of members of small GTPase Rab5 family. Unexpectedly, overexpression of the dominant-negative Rab5A mutant, Rab5A_S34N, did not eliminate the enlarged endosomes in this experimental model (data not shown). It may be that the overexpressed ALS2 peptide activates enough endogenous Rab5 GTPases or alternative downstream pathway(s) to permit endosomal enlargement.

To further strengthen our findings of ALS2rab5GEF activity, a dominant-negative form of the carboxy-terminus of EEA1 (EEA1_1270–1411 amino acids) (40), a well-characterized Rab5 downstream effector (28,41) was used. When EGFP–ALS2_660–1657 amino acids was co-expressed with FLAG–EEA1_1270–1411 amino acids, enlargement of

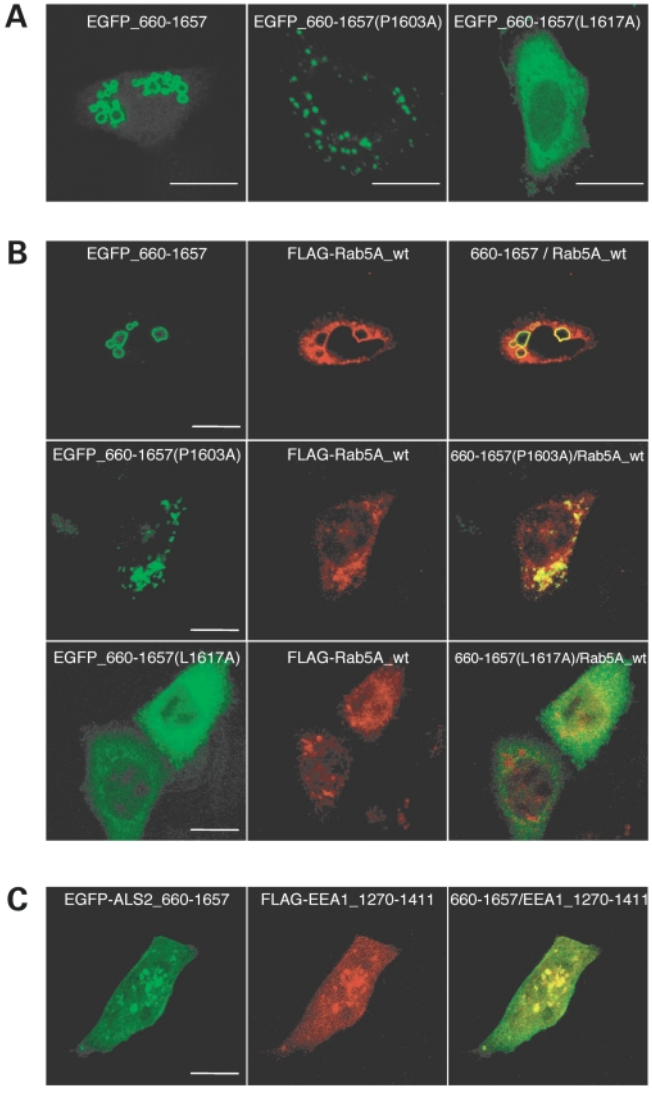

Figure 9. ALS2-promoted enlargement of endosomes is mediated by the activation of the Rab5–EEA1 pathway. (**A**) Effects of mutations in the VPS9 domain of the ALS2 protein on its intracellular distribution and endosome dynamics. Subcellular distribution of the ectopically expressed EGFP–ALS2_660–1657 (left), EGFP–ALS2_660–1657(P1603A) (middle) and EGFP–ALS2_660–1657 amino acids (L1617A) (right) in HeLa cells. (**B**) Co-expression of EGFP–ALS2_660–1657 (upper left), EGFP–ALS2_660–1657(P1603A) (middle left) or EGFP–ALS2_660–1657 amino acids (L1617A) (lower left) with FLAG–Rab5A_wt (middle) in HeLa cells. Merged images are shown in the right-hand columns. (**C**) Expression of the FLAG-tagged dominant-negative form of carboxy-terminal EEA1 fragment (FLAG–EEA1_1270–1411 amino acids) abrogates the ALS2-induced endosome enlargements. The left, middle and right columns display the images for EGFP–ALS2_660–1657, FLAG-EEA1_1270–1411 individually, and merged, respectively. Scale bars, 20 μm.

endosomes was completely suppressed (Fig. 9C). This indicates that ALS2rab5GEF involves inactivation of the Rab5–EEA1 pathway upstream of EEA1.

DISCUSSION

To our knowledge, the ALS2 protein is the fourth mammalian Rab5-specific GEF to be identified. The presence of a VPS9 domain in all four Rab5-GEFs (12–16) suggests that the essential GDP/GTP exchanging reaction may be conferred by this domain. A series of our deletion and mutagenesis studies revealed that the VPS9 domain of the ALS2 protein is a requisite for not only GDP/GTP exchange in Rab5 GTPase, but also endosomal targeting of the ALS2 protein. We have also demonstrated that the MORN motifs, although not essential for Rab5 binding, are necessary to fully activate ALS2rab5GEF. These data strongly suggests that VPS9 domain is working in conjunction with MORN co-operatively in the activation of the Rab5GTPases.

We have also documented the presence of regulatory elements and several GEF domains within the ALS2 molecule. The RLD appears to suppress recruitment of the full-length ALS2 protein onto endosomes and/or other membrane compartments in the cells. In contrast, the DH/PH domains appear to enhance MORN–VPS9 domain-mediated endosome fusion. A semi-quantitative analysis of the GDP dissociation *in vitro* revealed that the ALS2_660–1657 amino acid peptide containing DH/PH domains resulted in evident Rab5GEF activity which is significantly higher than that obtained with ALS2_1018–1657 amino acid peptide spanning a minimum region conferring the ALS2rab5GEF activity (Fig. 3C). This suggests that DH/PH could enhance ALS2rab5GEF activity resulting in a prominent endosome fusion. However, Rabex-5, a well-characterized Rab5-GEF (13,42), did not show significant endosome enlargement effects, despite its higher Rab5-GEF activity *in vitro* (Fig. 3C) and endosomal localization (Fig. 6B). We cannot rule out the possibility that the absence of endosome enlargement was due to insufficient levels of factors such as Rabaptin-5 known to interact with Rabex-5 (13,42). Nevertheless, it is clear that ALS2 and Rabex-5 proteins have differential effects on endosome dynamics in the cultured cells, suggesting that the multiple functional domains of the ALS2 protein in conjunction with unique upstream and/or downstream factors result in the leading of the intrinsic ALS2 function(s) and distribution.

Based on these results and endosomal dynamics (24,43–45), we propose the following physiological ALS2 function model (Fig. 10). Normally, RLD (RCC1-like domain) holds ALS2 proteins dispersed in the cytoplasm by means of an inter- and/or intra-RLD molecule association with the MORN-VPS9 region. In this situation, the majority of the cytosolic Rab5 molecules are maintained in GDP-bound inactive forms associated with Rab–GDI (GDP dissociation inhibitor) (46). An as yet unidentified molecular signal(s) inactivates RLD and activates MORN-VPS9 domain, initiating the recruitment of the ALS2 protein to the early endosomal compartments, where the ALS2 protein binds to a member of Rab5 small GTPases. The ALS2rab5GEF in the MORN-VPS9 domains of ALS2 then activates Rab5–GTPase through GDP/GTP exchange. The activated Rab5 further facilitates the formation of protein complex comprising downstream effector molecules such as EEA1 and SNARE (soluble *N*-ethylmaleimide-sensitive factor attachment protein receptor) proteins, promoting the endosomal fusion (47). Further, the ALS2 protein, particularly the DH/PH domain, could directly or indirectly up-regulate endosomal fusion.

Thus far, eight different mutations resulting in three distinct but phenotypically overlapping MNDs (ALS2, PLSJ and HSP)

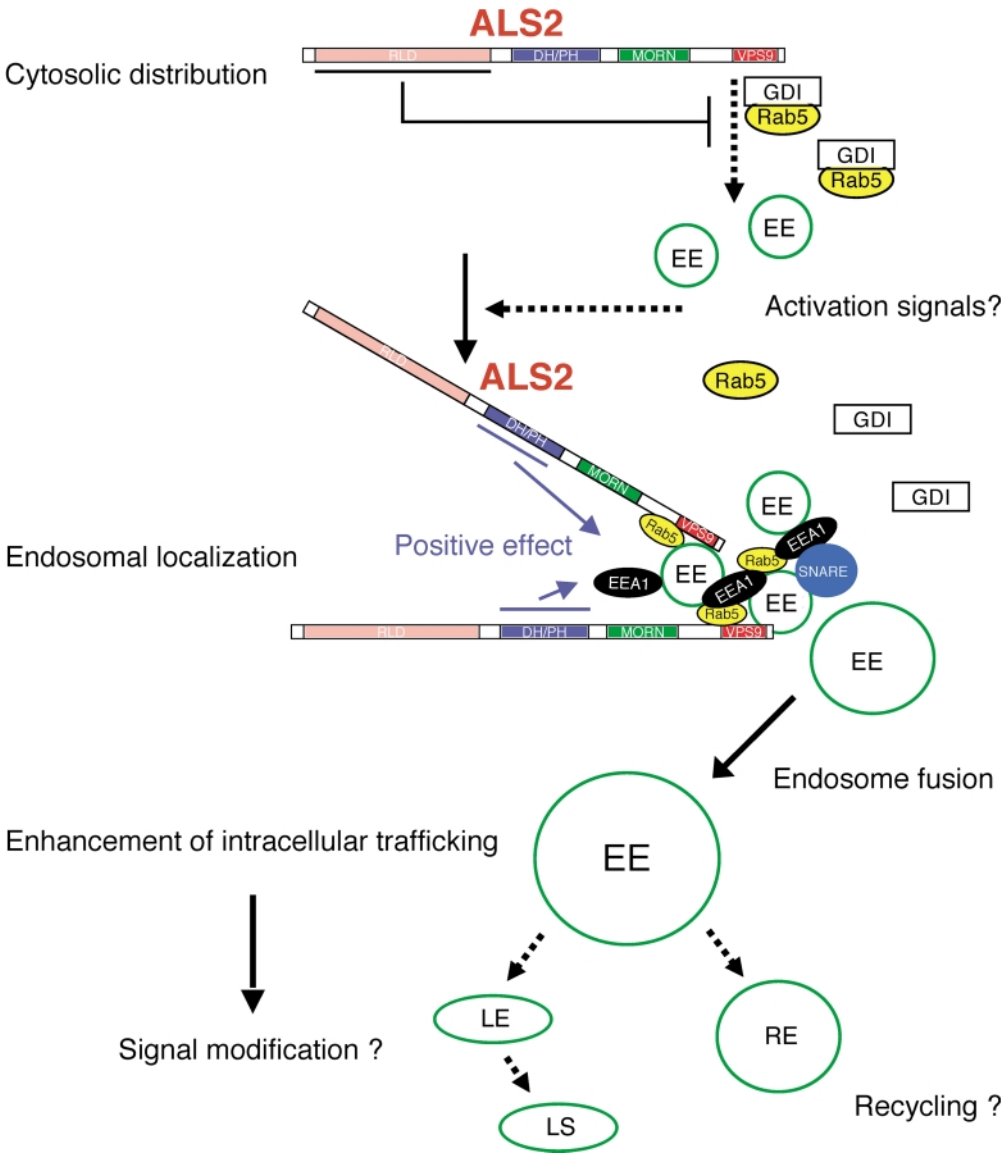

Figure 10. Proposed models for the ALS2 function and its implication in endosome dynamics. Pending a certain signal activation of the ALS2 molecule, RLD holds the ALS2 molecule dispersed in the cytoplasm by means of an inter- and/or intra-RLD molecule association with the MORN–VPS9 region. The majority of the Rab5 molecules exist in a GDP-bound inactive form associated with Rab–GDI. A particular molecular signal(s) (unidentified as yet) inactivates RLD and subsequently triggers MORN–VPS9 domains to recruit the ALS2 molecule for early endosomal compartments, wherein the ALS2 molecule binds to a member of Rab5 small GTPases. The ALS2rab5GEF in the MORN–VPS9 domains of the ALS2 protein activates Rab5–GTPase through GDP/GTP exchange. Activated Rab5 further facilitates the formation of protein complex comprising downstream effector molecules such as EEA1 and SNARE proteins, and promotes endosomal fusion. Further, the DH/PH domain could directly or indirectly up-regulate the fusion reactions. The ALS2 protein may also enhance certain intracellular transport of particular proteins and/or lipids and endosome-mediated signal transductions. In MND, loss of ALS2rab5GEF activity might disrupt endosomal trafficking and fusion, thereby resulting in the dysfunction and degeneration of the neuronal cells. GDI, Rab-GDP dissociation inhibitor; EEA1, early endosome antigen 1; SNARE, soluble *N*-ethylmaleimide-sensitive factor attachment protein receptor; EE, early endosome; LE, late endosome; RE, recycling endosome; LS, lysozome.

have been found in the *ALS2* gene (1,2,5,6). All the reported mutations cause disruption of the reading frame. A feature common to all ALS2–MND mutations is the loss of VPS9 domain, implicating ALS2rab5GEF function in endosome dynamics as being critical for motoneuron survival. This interpretation is consistent with the 4844delT mutation (4721delT; according to the den Dunnen's recommendations, www.DMD.nl/mutnomem.html) found in Pakistani kindred with HSP, which is predicted to result in a VPS9-functionless ALS2 protein, lacking half of the VPS9 domain at the carboxy-terminus (7). This *ALS2* gene mutation shows that loss of VPS9 domain (and loss of ALS2rab5GEF activity) is sufficient to

cause motor neuron death. The molecular mechanisms underlying phenotypic differences among ALS2, PLSJ and HSP, particularly LMN involvement, are still unclear at this stage. However, the uniform distribution of the short ALS2 protein variant both in cytoplasm and nucleus, which was completely different from those for the full-length ALS2 protein, could contribute to the phenotypic modulation.

Our functional model of the ALS2 protein may explain the unique molecular properties of the protein *in vivo*, and the selective or preferential dysfunction/degeneration of UMN resulting from the loss of rather widely expressed ALS2 proteins in patients with *ALS2* mutations. Notably, overexpression of the full-length ALS2 protein induced drastic enlargement of endosomes only in cultured neuronal cells, but not in HeLa or COS-7 cells. This suggests that a certain type of neuronal cell could be more amenable to the activation of the ALS2-mediated signaling pathways, and thus the devastating effects due to a loss of normal ALS2 protein could become more prominent in such neurons. Such a neuropathic effect of reduced or altered ALS2 function may involve the transport of neuronally specific macromolecules (e.g. proteins and/or lipids) or alter endosomally mediated signal transduction (48,49).

The recent identification of a number of causative genes has demonstrated that defective intracellular trafficking might underlie different forms of MNDs. In particular, the mutated genes for four types of HSPs, including SPG3A (50), SPG4 (51), SPG10 (52) and SPG20 (53), are all thought to directly involve intracellular trafficking (50–55). In addition, mutations in *KIF1B*β, which encodes a kinesin motor protein, and Rab7 result in Charcot–Marie–Tooth type 2A (OMIM 118210) (56) and type 2B (OMIM 600882) (57), respectively. Both are common inherited peripheral neuropathies. Defects in axonal transport and cytoskeletal organization have also been seen in sporadic as well as some familial ALS (58,59). Combining these result with our findings that the ALS2 protein functions as Rab5–GEF (ALS2rab5GEF), malfunction of the ALS2rab5GEF could obstruct membrane organization and endosomal dynamics, including endosome trafficking and fusion, and is implicated in ALS2, PLSJ and HSP.

MATERIALS AND METHODS

Antibodies

Anti-ALS2 rabbit antisera were raised by immunizing Japanese White rabbits with peptide (HPP1024; human ALS2 1024–1040 amino acids: QRQEPPISRSAKYTFYK) coupled to keyhole limpet hemocyanin via an amino-terminal cysteine residue, or with the purified His-tagged human ALS2_RLD fragment (HPF1-680; 1–680 amino acids). Each polyclonal antibody was affinity-purified using an antigen-coupled sepharose column. Other antibodies used in this study included anti-Flag monoclonal antibody M2 (1:3000; Stratagene), anti-GST monoclonal antibody (1:3000; Santa Cruz), anti-Rab4 monoclonal antibody (1:1000; Transduction Laboratories), anti-Rab5 monoclonal antibody (1:1000; Transduction Laboratories), anti-Rab11 monoclonal antibody (1:500; Transduction Laboratories), anti-EEA1 monoclonal antibody (1:100; BD biosciences), anti-GM130 monoclonal antibody (1:500; BD biosciences), anti-LAMP-1 monoclonal antibody (1:100; BD biosciences), anti-LAMP-2 monoclonal antibody (1:250; BD biosciences), anti-Tau monoclonal antibody (1:100; CalBioChem) and anti-β-tubulin monoclonal antibody (1:20 000; CHEMICON).

Western blot analysis

Whole-tissue extracts were prepared from fresh mouse tissues by homogenizing in lysis buffer [25 mM Tris–HCl; pH 7.5, 5 mM $MgCl_2$, 50 mM NaCl, 1 mM dithiothreitol (DTT), 5% (w/v) sucrose, 1% (w/v) IGIPAL CA-630, protease inhibitor cocktail (Roche), 1 mM phenylmethylsulfonyl fluoride (PMSF)], denatured in SDS sample buffer, subjected to SDS–PAGE, and transferred onto a PVDF membrane. Protein samples for the human cerebral cortex and cerebellum were purchased from BIOCHAIN Inc. Blots were incubated with anti-ALS2 antibodies (1:2000) or anti-β-tubulin antibody for 2 h, and with horseradish peroxidase-conjugated anti-rabbit or anti-mouse IgG sheep secondary antibody (Amersham Pharmacia), and developed using the ECL-plus kit (Amersham Pharmacia).

Plasmid constructs

All cDNA clones used in this study were obtained by reverse transcription with polymerase chain reaction (RT–PCR) from human brain or heart total RNA, followed by subcloning into the appropriate expression vectors (see below). The DNA sequence of the insert as well as the flanking regions in each cDNA clone was verified by sequencing. Numbers in the designated ALS2 clones correspond to the encoded amino acids of the ALS2 or EEA1 protein. Mutant constructs harboring point mutations were generated by oligonucleotide-directed mutagenesis using GeneEditor™ *in vitro* Site-Directed Mutagenesis System (Promega) according to the manufacturer's instructions.

ALS2 construct for antibody generation. The RLD region, encoding amino acids 1–680, was subcloned into pRSET Bacterial Expression Vector (Invitrogen), generating pRSETHis-ALS2_1–680.

ALS2 and Rabex-5 constructs for GDP/GTP exchange and in vitro *binding assays.* A total of eight cDNA fragments (one encoding full-length *ALS2*, six encoding truncated *ALS2* fragments and one encoding *RABEX5*) were subcloned into the modified pCI-neo Mammalian Expression Vector (Promega), allowing the production of amino-terminally FLAG-tagged proteins. Constructs were as follows: pCIneoFLAG–ALS2_L (full-length); pCIneoFLAG–ALS2_660–1657, pCIneoFLAG–ALS2_913–1657; pCIneoFLAG–ALS2_1018–1657; pCIneoFLAG–ALS2_1251–1657; pCIneoFLAG–ALS2_1351–1657; pCIneoFLAG–ALS2_1–1275; and pCIneoFLAG–Rabex5. Finally, two

constructs harboring different point mutations were generated: pCIneoFLAG–ALS2_660–1657(P1603A) and pCIneoFLAG–ALS2_660–1657(L1617A).

ALS2 constructs for in vitro *GST-pull down assay.* Three fragments of the *ALS2* cDNA were subcloned into pGEX–6P (Amersham Pharmacia) Bacterial expression vector, generating pGEX6P–ALS2_1018–1657, pGEX6P–ALS2_1251–1657 and pGEX6P–ALS2_1351–1657.

Small GTPase constructs for GDP/GTP exchange and in vitro *binding assays.* A total of 14 cDNA fragments encoding 14 different small GTPases, including ARF1, ARF6, Rab3A, Rab4A, Rab5A, Rab5B, Rab5C, Rab7, Rab9A, Rab11A, Ran, Rac1, RhoA and Cdc42, were subcloned into pGEX-6P bacterial expression vector (Amersham Pharmacia). The resulting constructs included pGEX6P–ARF1, pGEX6P–ARF6, pGEX6P–Rab3A, pGEX6P–Rab4A, pGEX6P–Rab5A, pGEX6P–Rab5B, pGEX6P–Rab5C, pGEX6P–Rab7, pGEX6P–Rab9A, pGEX6P–Rab11A, pGEX6P–Ran, pGEX6P–Rac1, pGEX6P–RhoA and pGEX6P–Cdc42.

Constructs for the localization studies. Full-length (ALS2_L), short form (ALS2_S) and four deletion fragments derived from the *ALS2* cDNA, and six small GTPases cDNA fragments, were subcloned into pCI-neo (Promega), pEGFP-C1 (Clontech) or p3XFLAG-CMV^{TM}-10 Expression Vector (Sigma), generating pCIneo–ALS2_L, pCIneo–ALS2_S, pEGFP–ALS2_L, pEGFP–ALS2_1–680, pEGFP–ALS2_660–1657, pEGFP–ALS2_1018–1657, pEGFP–ALS2_1351–1657, p3XFLAG–CMV10–Rab5A, p3XFLAG–CMV10–Rab5AQ79L, p3XFLAG–CMV10–Rab5AS34N, p3XFLAG–CMV10–Rab4A, p3XFLAG–CMV10–Rab7 and p3XFLAG–CMV10–Rab11A. To generate the EGFP–ALS2 constructs harboring a point mutation, the mutated *ALS2* inserts were excised from pCIneoFLAG–ALS2_660–1657(P1603A) and pCIneoFLAG–ALS2_660–1657(L1617A), and subcloned into pEGFP-C1 vector (Clontech), generating pEGFP–ALS2_660–1657(P1603A) and pEGFP–ALS2_660–1657(L1617A), respectively. Dominant negative EEA1 expression construct consisting of the carboxy-terminal fragment of EEA1 (p3XFLAG–CMV10–EEA1_1270–1411) was also generated.

Cell culture and transfection

HeLa and COS-7 cells were cultured in Dulbecco's modified Eagle's medium (DMEM) supplemented with 10% heat-inactivated fetal bovine serum (Invitorogen), 100 U/ml penicillin and 100 µg/ml streptpmycin. Primary neuronal cell cultures were established from cerebral cortex derived from embryos at 18 days (E18) of Sprague–Dawley rat according to the methods as previously described (60). HeLa/COS-7 cells and primary neuronal cells were transfected with plasmid constructs using the Effectene Transfection Reagent (Qiagen) and the LipofectAMINE 2000 (Invitrogen), respectively, according to the manufacturer's instructions.

Preparation of ALS2 and Rabex-5

COS-7 cells were transfected with pCIneo-FLAG constructs. Cells were lysed in TBST buffer [50 mM Tris–HCl; pH 7.4, 150 mM NaCl, 1 mM EDTA, 2% (w/v) Tween-20] for 3 h at 4°C, and centrifuged at 12 000*g* for 15 min at 4°C. Supernatants were immmunoprecipitated using EZview^{TM} Red ANTI-FLAG® M2 Affnity Gel (Sigma) according to the manufacturer's instructions. The amino-terminally FLAG-tagged ALS2 and Rabex-5 proteins bound to gel beads were re-suspended in appropriate volumes of GEF buffer (25 mM Tris–HCl; pH 7.4, 50 mM NaCl, 20 mM $MgCl_2$, 1 mM CHAPS), and used for GDP/GTP exchange assay *in vitro.* A portion of the proteins was subjected to SDS–PAGE, followed by western blotting analysis with anti-FLAG antibody to estimate the amounts of conjugating FLAG-tagged proteins on the beads.

Purification of small GTPases

GST-fusion small GTPases and GST-fusion ALS2 proteins were expressed in *E. coli* BL21(DE3)pLys S (Novagen) transformed with each pGEX6P2 construct, and purified using the glutathione–Sepharose^{TM} 4B beads (Amersham Pharmacia) according to the manufacturer's instructions. GST-fusion ALS2 proteins were used for *in vitro* binding assay. For small GTPases, GST-fusion proteins were further treated with PreScission protease (Amersham Pharmacia) to remove the GST moiety according to the manufacturer's recommendations. The resulting purified small GTPases were utilized in either GDP/GTP exchange assay or *in vitro* binding assay.

In vitro GDP/GTP exchange assay

[^{3}H]GDP dissociation assay. Each purified small GTPase (200 pmol) was loaded with [^{3}H]GDP (0.8 nmol; 370 Gbq/mmol; Amersham Pharmacia) in GXP loading buffer (25 mM Tris–HCl; pH 7.5, 50 mM NaCl, 10 mM EDTA, 5 mM $MgCl_2$, 1 mM DTT, 1 mM CHAPS) for 30 min at 30°C. To stabilize nucleotide binding, $MgCl_2$ was added to a final concentration of 20 mM, and the mixture cooled to 4°C. The GDP-loaded proteins were then purified by PD-10 column (Amersham Pharmacia) in GEF buffer. Four picomoles of the [^{3}H]GDP loaded small GTPase were pre-incubated for 5 min at 30°C, and nucleotide dissociation reaction was initiated by the addition of gel beads conjugating 2 pmol equivalent of the immunoprecipitated FLAG-tagged ALS2 or Rabex-5 protein, and further incubated for the indicated durations of time at 30°C in a final volume of 40 µl GEF buffer in the presence of 5 mM GTP. Reactions were then terminated by adding excess volume of ice-cold STOP buffer (25 mM Tris–HCl; pH 7.5, 100 mM NaCl, 20 mM $MgCl_2$), and filtered through BA85 nitrocellurose filters (Schleicher & Schell). The radioactivity trapped on the filters was counted.

[^{35}S]GTPγS binding assay. Rab5A was preloaded with either GTPγS or GDP essentially in the same manner as above. Gel beads conjugating 2 pmol equivalent of the immunoprecipitated FLAG-tagged ALS2 protein and 0.5 pmol of [^{35}S]GTPγS (37 Tbq/mmol; Amersham Pharmacia) were pre-incubated for 5 min at 30°C. Reactions were initiated by the addition of

4 pmol of Rab5A–GDP, Rab5A–GTPγS, or nucleotide-free Rab5A, and incubated for the indicated duration of time at 30°C in a final volume of 40 µl GEF buffer. Reactions were then terminated and filtered, followed by scintillation counting.

In vitro binding assay

Purified Rab5A (4 pmol), which was pre-loaded with either GDP or GTPγS, or nucleotide-free, was mixed with FLAG-M2 beads conjugating 4 pmol equivalent of the immunoprecipitated FLAG-tagged ALS2 in 100 µl of GEF buffer containing 0.1% skimmed milk for 2 h at 30°C. After washing with 4 × 1 ml of GEF buffer, the bound Rab5A was co-eluted with FLAG-ALS2 protein by the addition of SDS–PAGE sample buffer, and detected by western blotting analysis using appropriate antibodies. For GST pull-down experiments, purified small GTPases (0.3 pmol), Rab4A, Rab5A and Rab11A, which were pre-loaded with either GDP or GTPγS, or nucleotide-free, were mixed with glutathione–Sepharose 4B beads coated with 10 pmol of GST, GST–ALS2_1018–1657, GST–ALS2_1251–1657, or GST–ALS2_1351–1657 in 1 ml of binding buffer (20 mM HEPES; pH 7.4, 50 mM NaCl, 10 mM $MgCl_2$, 1 mM DTT, 0.05% Triton X-100, 100 µM GDP or GTPγS) for 1.5 h at 25°C. After washing with 4 × 1 ml of washing buffer (20 mM HEPES; pH 7.4, 100 mM NaCl, 10 mM $MgCl_2$, 1 mM DTT, 0.05% Triton X-100, 10 µM GDP or GTPγS), the bound small GTPases were co-eluted with GST fusion proteins by the addition of SDS–PAGE sample buffer, and detected by western blotting analysis using appropriate antibodies.

Immunofluorescence study

The transfected cells were washed with PBS(−) twice, fixed with 4% paraformaldehyde (PFA) in PBS(−) (pH 7.5) for 30 min at room temperature, and permeabilized with 0.5% (w/v) TritonX-100 in PBS(−) for 30 min. The primary antibodies, diluted in PBS(−) containing 1.5% normal goat serum and 0.05% TritonX-100, were added to cells and incubated for 2 h at room temperature. Alexa 594-conjugated goat anti-mouse IgG (1:200; Molecular Probes) or Alexa 594-conjugated goat anti-rabbit IgG (1:500; Molecular Probes) was used for the detection of the signals of either the tag epitope or proteins of interest. In neuronal cultured cells, ALS2 was detected by probing with anti-ALS2 polyclonal antibody (HPF1-680) and Alexa 488-conjugated anti-rabbit IgG (1:500; Molecular Probes), while Tau was visualized by staining with anti-Tau monoclonal antibody, followed by Alexa 594-conjugated goat anti-mouse IgG (1:200; Molecular Probes).

Uptake of endocytic tracers

For labeling with transferrin, HeLa cells were washed with PBS(−) twice and incubated in serum-free medium for 30 min at 37°C in 5% CO_2, followed by the incubation with serum-free medium containing 25 µg/ml transferrin Alexa 594 conjugates (Molecular Probes) for an additional 30 min at 37°C. Then, the cells were rapidly chilled with ice-cold PBS(−) and fixed with 4% PFA. For labeling with epidermal growth factor (EGF), HeLa cells were incubated with serum-free medium containing 1% BSA for 30 min at 37°C, and then incubated with fresh serum free medium containing 2.5 µg/ml EGF-tetramedtylrhodamine conjugates (Molecular Probes) for additional 30 min at 37°C. After labeling, the cells were washed and fixed in the same manner as used in transferrin labeling.

Light and confocal microscopies

Images of serial optical sections with 1–2.5 µm thickness were captured and analyzed by Leica TCS_NT confocal-microscope systems (Leica).

Immunohistochemistry

Formalin-fixed human brain samples were embedded in paraffin, and sectioned with 7 µm thickness for immunohistochemistry. Immunostaining for the ALS2 protein was performed with the affinity-purified anti-ALS2_RLD polyclonal antibody (HPF1–680) using a Vectastain elite ABC kit (Vector Lab) according to the manufacturer's recommendations.

ACKNOWLEDGEMENTS

We thank Dr A.E. MacKenzie at Ottawa University for the critical reading of the manuscript, and all the members of our laboratory for helpful discussion and suggestions. This work was founded by the Japan Science and Technology Corporation (JST) (to J.-E.I.) and the Ministry of Health, Labour and Welfare (to J.-E.I.). A part of this work was supported by a Grant-in-Aide for Scientific Research on Priority(C)—Advanced Brain Science Project from Ministry of Education, Culture, Sports, Science, and Technology, Japan (to J.-E.I.), a Grant-in-Aide for Scientific Research from Japan Society for the Promotion of Science (to S.H.), the Sumitomo Foundation (to S.H.), Kihara Memorial Yokohama Foundation for the Advancement of Life Sciences (to S.H.), and the Ichiro Kanehara Foundation (to S.H.).

REFERENCES

1. Hadano, S., Hand, C.K., Osuga, H., Yanagisawa, Y., Otomo, A., Devon, R.S., Miyamoto, N., Showguchi-Miyata, J., Okada, Y., Singaraja, R. *et al.* (2001) A gene encoding a putative GTPase regulator is mutated in familial amyotrophic lateral sclerosis 2. *Nat. Genet.*, **29**, 166–173.
2. Yang, Y., Hentati, A., Deng, H.X., Dabbagh, O., Sasaki, T., Hirano, M., Hung, W.Y., Ouahchi, K., Yan, J., Azim, A.C. *et al.* (2001) The gene encoding alsin, a protein with three guanine–nucleotide exchange factor domains, is mutated in a form of recessive amyotrophic lateral sclerosis. *Nat. Genet.*, **29**, 160–165.
3. Ben Hamida, M., Hentati, F. and Ben Hamida, C. (1990) Hereditary motor system diseases (chronic juvenile amyotrophic lateral sclerosis). *Brain*, **113**, 347–363.
4. Lerman-Sagie, T., Filiano, J., Smith, D.W. and Korson, M. (1996) Infantile onset of hereditary ascending spastic paralysis with bulbar involvement. *J. Child. Neurol.*, **11**, 54–57.
5. Eymard-Pierre, E., Lesca, G., Dollet, S., Santorelli, F.M., di Capua, M., Bertini, E., Boespflug-Tanguy, O. *et al.* (2002) Infantile-onset ascending hereditary spastic paralysis is associated with mutations in the alsin gene. *Am. J. Hum. Genet.*, **71**, 518–527.
6. Lesca, G., Eymard-Pierre, E., Santorelli, F.M., Cusmai. R., Di Capua, M., Valente, E.M., Attia-Sobol, J., Plauchu, H., Leuzzi, V., Ponzone, A. *et al.* (2003) Infantile ascending hereditary spastic paralysis (IAHSP): Clinical features in 11 families. *Neurology*, **60**, 674–682.

7. Gros-Louis, F., Meijer, I.A., Hand, C.K., Dube, M.P., MacGregor, D.L., Seni, M.H., Devon, R.S., Hayden, M.R., Andermann, F., Andermann, E. *et al.* (2003) An *ALS2* gene mutation causes hereditary spastic paraplegia in a Pakistani kindred. *Ann. Neurol.*, **53**, 144–145.
8. Leavitt, B.R. and Brunham, L.R. (2002) Hereditary motor neuron disease caused by mutations in the ALS2 gene: the long and the short of it. *Clin. Genet.*, **62**, 265–269.
9. Ohtsubo, M., Kai, R., Furuno, N., Sekiguchi, T., Sekiguchi, M., Hayashida, H., Kuma, K., Miyata, T., Fukushige, S. Murotsu, T. *et al.* (1987) Isolation and characterization of the active cDNA of the human cell cycle gene (RCC1) involved in the regulation of onset of chromosome condensation. *Genes Dev.*, **1**, 585–593.
10. Rosa, J.L. Casaroli-Marano, R.P., Buckler, A.J. Vilaró, S. and Barbacid, M. (1996) p532, a giant protein related to the chromosome condensation regulator RCC1, stimulates guanine nucleotide exchange on ARF1 and Rab proteins. *EMBO J.*, **15**, 4262–4273.
11. Schmidt, A. and Hall, A. (2002) Guanine nucleotide exchange factors for Rho GTPases: turning on the switch. *Genes Dev.*, **16**, 1587–1609.
12. Burd, C.G., Mustol, P.A., Schu, P.V. and Emr, S.D. (1996) A yeast protein related to a mammalian Ras-binding protein, Vps9p, is required for localization of vacuolar proteins. *Mol. Cell. Biol.*, **16**, 2369–2377.
13. Horiuchi, H., Lippe, R., McBride, H.M., Rubino, M., Woodman, P., Stenmark, H., Rybin, V., Wilm, M., Ashman, K., Mann, M. *et al.* (1997) A novel Rab5 GDP/GTP exchange factor complexed to Rabaptin-5 links nucleotide exchange to effector recruitment and function. *Cell*, **90**, 1149–1159.
14. Han, L., Wong, D., Dhaka, A., Afar, D., White, M., Xie, W., Herschman, H., Witte, O. and Colicelli, J. (1997) Protein binding and signaling properties of RIN1 suggest a unique effector function. *Proc. Natl Acad. Sci. USA*, **94**, 4954–4959.
15. Tall, G.G., Barbieri, M.A., Stahl, P.D. and Horazdovsky, B.F. (2001) Ras-activated endocytosis is mediated by the Rab5 guanine nucleotide exchange activity of RIN1. *Dev. Cell*, **1**, 73–82.
16. Saito, K., Murai, J., Kajiho, H., Kontani, K., Kurosu, H. and Katada, T. (2002) A novel binding protein composed of homophilic tetramer exhibits unique properties for the small GTPase Rab5. *J. Biol. Chem.*, **277**, 3412–3418.
17. Takeshima, H., Komazaki, S., Nishi, M., Iino, M. and Kangawa, K. (2000) Junctophilins: a novel family of junctional membrane complex proteins. *Mol. Cell*, **6**, 11–22.
18. Dasso, M. (2001) Running on Ran: nuclear transport and the mitotic spindle. *Cell*, **104**, 321–324.
19. Etienne-Manneville, S. and Hall, A. (2002) Rho GTPases in cell biology. *Nature*, **420**, 629–635.
20. Van Aelst, L. and Symons, M. (2002) Role of Rho family GTPases in epithelial morphogenesis. *Genes Dev.*, **16**, 1032–1054.
21. Snider, W.D., Zhou, F.-Q., Zhong, Z. and Markus, A. (2002) Signaling the pathway to regeneration. *Neuron*, **35**, 13–16.
22. Luo, L. (2000) Rho GTPases in neuronal morphogenesis. *Nat. Rev. Neurosci.*, **1**, 173–180.
23. Da Silva, J.S. and Dotti, C.G. (2002) Breaking the neuronal sphere: regulation of the actin cytoskeleton in neuritogenesis. *Nat. Rev. Neurosci.*, **3**, 694–704.
24. Zerial, M. and McBride, H. (2001) Rab proteins as membrane organizers. *Nat. Rev. Mol. Cell Biol.*, **2**, 107–117.
25. Vetter, I.R. and Wittinghofer, A. (2001) The guanine-nucleotide-binding switch in three dimensions. *Science*, **294**, 1299–1304.
26. Jensen, R.B., La Cour, T., Albrethsen, J., Nielsen, M. and Skriver, K. (2001) FYVE zinc-finger proteins in the plant model *Arabidopsis thaliana*: identification of PtdIns3*P*-binding residues by comparison of classic and variant FYVE domains. *Biochem. J.*, **359**, 165–173.
27. Mu, F.T., Callaghan, J.M., Steele-Mortimer, O., Stenmark, H., Parton, R.G,. Campbell, P.L., McCluskey, J., Yeo, J.P., Tock, E.P., Toh, B.H. *et al.* (1995) EEA1, an early endosome-associated protein: EEA1 is a conserved alpha-helical peripheral membrane protein flanked by cysteine 'fingers' and contains a calmodulin-binding IQ motif. *J. Biol. Chem.*, **270**, 13503–13511.
28. Christoforidis, S., McBride, H.M., Burgoyne, R.D. and Zerial, M. (1999) The Rab5 effector EEA1 is a core component of endosome docking. *Nature*, **397**, 621–625.
29. Wilson, J.M., de Hoop, M., Zorzi, N., Toh, B.-H., Dotti, C.G. and Parton, R.G. (2000) EEA1, a tethering protein of the early sorting endosome, shows a polarized distribution in hippocampal neurons, epithelial cells, and fibroblasts. *Mol. Biol. Cell*, **11**, 2657–2671.
30. Stenmark, H., Parton, R.G., Steele-Mortimer, O., Lutcke, A., Gruenberg, J. and Zerial, M. (1994) Inhibition of rab5 GTPase activity stimulates membrane fusion in endocytosis. *EMBO J.*, **13**, 1287–1296.
31. Sönnichsen, B., De Renzis, S., Nielsen, E., Rietdorf, J. and Zerial, M. (2000) Distinct membrane domains on endosomes in the recycling pathway visualized by multicolor imaging of Rab4, Rab5, and Rab11. *J. Cell Biol.*, **149**, 901–913.
32. Bucci, C., Parton, R.G., Mather, I.H., Stunnenberg, H., Simons, K., Hoflack, B. and Zerial, M. (1992) The small GTPase rab5 functions as a regulatory factor in the early endocytic pathway. *Cell*, **70**, 715–728.
33. Bottger, G., Nagelkerken, B. and van der Sluijs, P. (1996) Rab4 and Rab7 define distinct nonoverlapping endosomal compartments. *J. Biol. Chem.*, **271**, 29191–29197.
34. Bucci, C., Thomsen, P., Nicoziani, P., McCarthy, J. and van Deurs, B. (2000) Rab7: a key to lysosome biogenesis. *Mol. Biol. Cell*, **11**, 467–480.
35. Ullrich, O., Reinsch, S., Urbe, S., Zerial, M. and Parton, R.G. (1996) Rab11 regulates recycling through the pericentriolar recycling endosome. *J. Cell. Biol.*, **135**, 913–924.
36. Barr, F.A., Nakamura, N. and Warren, G. (1998) Mapping the interaction between GRASP65 and GM130, components of a protein complex involved in the stacking of Golgi cisternae. *EMBO J.*, **17**, 3258–3268.
37. Fukuda, M. (1994) Biogenesis of the lysosomal membrane. *Subcell. Biochem.*, **22**, 199–230.
38. Howe, C.L., Granger, B.L., Hull, M., Green, S.A., Gabel, C.A., Helenius, A. and Mellman, I. (1988) Derived protein sequence, oligosaccharides, and membrane insertion of the 120-kDa lysosomal membrane glycoprotein (lgp120): identification of a highly conserved family of lysosomal membrane glycoproteins. *Proc. Natl Acad. Sci. USA*, **85**, 7577–7581.
39. Rosenfeld, J.L., Moore, R.H., Zimmer, K.P., Alpizar-Foster, E., Dai, W., Zarka, M.N. and Knoll, B.J. (2001) Lysosome proteins are redistributed during expression of a GTP-hydrolysis-defective rab5a. *J. Cell Sci.*, **114**, 4499–4508.
40. Lawe, D.C., Patki, V., Heller-Harrison, R., Lambright, D. and Corvera, S. (2000) The FYVE domain of early endosome antigen 1 is required for both phosphatidylinositol 3-phosphate and Rab5 binding. Critical role of this dual interaction for endosomal localization. *J. Biol. Chem.*, **275**, 3699–3705.
41. Simonsen, A., Lippe, R., Christoforidis, S., Gaullier, J.M., Brech, A., Callaghan, J., Toh, B.H., Murphy, C., Zerial, M., Stenmark, H. *et al.* (1998) EEA1 links PI(3)K function to Rab5 regulation of endosome fusion. *Nature*, **394**, 494–498.
42. Lippé, R., Miaczynska, M., Rybin, V., Runge, A. and Zerial, M. (2001) Functional synergy between Rab5 effector Rabaptin-5 and exchange factor Rabex-5 when physically associated in a complex. *Mol. Biol. Cell*, **12**, 2219–2228.
43. Katzmann, D.J., Odorizzi, G. and Emr, S.D. (2002) Receptor down-regulation and multivesicular-body sorting. *Nat. Rev. Mol. Cell Biol.*, **3**, 893–905.
44. De Renzis, D., Sönnichsen, B. and Zerial, M. (2002) Divalent Rab effectors regulate the sub-compartmental organization and sorting of early endosomes. *Nat. Cell Biol.*, **4**, 124–133.
45. Gruenberg, J. (2001) The endocytic pathway: a mosaic of domains. *Nat. Rev. Mol. Cell Biol.*, **2**, 721–730.
46. Pfeffer, S.R., Dirac-Svejstrup, A.B. and Soldati, T. (1995) Rab GDP dissociation inhibitor: putting Rab GTPases in the right place. *J. Biol. Chem.*, **270**, 17057–17059.
47. McBride, H.M., Rybin, V., Murphy, C., Giner, A., Teasdale, R. and Zerial, M. (1999) Oligomeric complexes link Rab5 effectors with NSF and drive membrane fusion via interactions between EEA1 and Syntaxin 13. *Cell*, **98**, 377–386.
48. Panopoulou, E., Gillooly, D.J., Wrana, J.L., Zerial, M., Stenmark, H., Murphy, C. and Fotsis, T. (2002) Early endosomal regulation of Smad-dependent signaling in endothelial cells. *J. Biol. Chem.*, **277**, 18046–18052.
49. Clague, M.J. and Urbé, S. (2001) The interface of receptor trafficking and signaling. *J. Cell Sci.*, **114**, 3075–3081.
50. Zhao, X., Alvarado, D., Rainier, S., Lemons, R., Hedera, P., Weber, C.H., Tukel, T., Apak, M., Heiman-Patterson, T., Ming, L. *et al.* (2001) Mutations in a newly identified GTPase gene cause autosomal dominant hereditary spastic paraplegia. *Nat. Genet.*, **29**, 326–331.
51. Hazan, J., Fonknechten, N., Mavel, D., Paternotte, C., Samson, D., Artiguenave, F., Davoine, C.S., Cruaud, C., Durr, A., Wincker, P. *et al.* (1999) Spastin, a new AAA protein, is altered in the most frequent form of autosomal dominant spastic paraplegia. *Nat. Genet.*, **23**, 296–303.

52. Reid, E., Kloos, M., Ashley-Koch, A., Hughes, L., Bevan, S., Svenson, I.K., Graham, F.L., Gaskell, P.C., Dearlove, A., Pericak-Vance, M.A. *et al.* (2002) A kinesin heavy chain (*KIF5A*) mutation in hereditary spastic paraplegia (SPG10). *Am. J. Hum. Genet.*, **71**, 1189–1194.
53. Patel, H., Cross, H., Proukakis, C., Hershberger, R., Bork, P., Ciccarelli, F.D, Patton, M.A., McKusick, V.A. and Crosby, A.H. (2002) *SPG20* is mutated in Troyer syndrome, an hereditary spastic paraplegia. *Nat. Genet.*, **31**, 347–348.
54. Brownlees, J., Ackerley, S., Grierson, A.J., Jacobsen, N.J., Shea, K., Anderton, B.H., Leigh, P.N., Shaw, C.E. and Miller, C.C. (2002) Charcot-Marie-Tooth disease neurofilament mutations disrupt neurofilament assembly and axonal transport. *Hum. Mol. Genet.*, **11**, 2837–2844.
55. Crosby, A.H. and Proukakis, C. (2002) Is the transportation highway the right road for hereditary spastic paraplegia? *Am. J. Hum. Genet.*, **71**, 1009–1016.
56. Zhao, C., Takita, J., Tanaka, Y., Setou, M., Nakagawa, T., Takeda, S., Yang, H.W., Terada, S., Nakata, T., Takei, Y. *et al.* (2001) Charcot-Marie-Tooth disease type 2A caused by mutation in a microtubule motor KIF1Bβ. *Cell*, **105**, 587–597.
57. Verhoeven, K., De Jonghe, P., Coen, K., Verpoorten, N., Auer-Grumbach, M., Kwon, J.M., FitzPatrick, D., Schmedding, E., De Vriendt, E., Jacobs, A., Van Gerwen. V. *et al.* (2003) Mutations in the small GTP-ase late endosomal protein RAB7 cause Charcot–Marie–Tooth type 2B neuropathy. *Am. J. Hum. Genet.*, **72**, 722–727.
58. Cleveland, D.W. and Rothstein, J.D. (2001) From Charcot to Lou Gehrig: deciphering selective motor neuron death in ALS. *Nat. Rev. Neurosci.*, **2**, 806–819.
59. Julien, J.-P. (2001) Amyotrophic lateral sclerosis: unfolding the toxicity of the misfolded. *Cell*, **104**, 581–591.
60. Bito, H., Furuyashiki, T., Ishihara, H., Shibasaki, Y., Ohashi, K., Mizuno, K., Maekawa, M., Ishizaki, T. and Narumiya, S. (2000) A critical role for a Rho-associated kinase, p160ROCK, in determining axon outgrowth in mammalian CNS neurons. *Neuron*, **26**, 431–441.